THE UNIVERSITY OF QUEENSLAND

Dynamic Wireless Charging System for an Autonomous Electric Hauler

Student Name: William HALE

Course Code: ENGG7290

Academic Supervisor: Professor Chandima Ekanayake

Placement Company/Institution: Mining3

Submission Date: 27 June 2019

Executive Summary

The fundamental appeal for wireless charging is the ability to deliver power to electrical systems without the use of cables and wires. Mobiles, laptops, electric cars, and other systems which run on electricity posses the need to be plugged in and charged. Static wireless charging removes the requirement for cables, however, to statically charge an electrical system, it must still be removed from operation.

Alternatively, dynamic wireless charging provides another level of convenience. If an electrical system could obtain all necessary power whilst operating, the system would never require removal from operation. The aim of this research was to develop a dynamic wireless charging system for an autonomous electric mining vehicle. The long-term objective motivating this research is the development of electric mining vehicles which can operate indefinitely by sourcing power wirelessly whilst in operation.

The first phase of the project was to conduct a literature review, and collate state-of-the-art systems regarding dynamic wireless power transfer. It was found that a resonant inductive wireless power transfer system was the optimal topology for electric vehicle charging. This is because a resonant system can maintain strong coupling over significant air gaps (several coil diameters wide). Other key findings were that winding charging coils with Litz wire, and utilizing both magnetic and metallic shielding could greatly improve the efficiency of the wireless power transfer.

During the research phase, it was also discovered that when developing a dynamic wireless charging system, there are more design considerations than just the system's efficiency and power transfer capabilities over an air gap. A major design consideration for the dynamic system is how robust the wireless power transfer is to misalignments between the transmitter and receiver. As the electric vehicle sources power wirelessly by driving over a series of transmitter pads (a transmitter network), there is always some level of misalignment between the receiver module on the vehicle, and the transmitter pads on the ground.

Through further research, inductive coupling simulations using ANSYS, and small-scale prototyping, conclusions were drawn regarding the optimal system for the dynamic wireless charging of an electric vehicle. It was recommended that future research should investigate a "crossed DD pad" transmitter network design, a "DDQ pad" receiver module design, and a resonance tuning feedback network which can respond quickly to changes in misalignment. A system which utilizes the aforementioned recommendations would likely become very robust to any type of misalignment between the transmitter and receiver. It was also recommended that a segmentation system should be implemented which uses an optical sensing technique, as opposed to magnetic sensing.

Acknowledgements

First and foremost, I would like to thank Mining3 for providing this incredible opportunity, and my workplace supervisor, Dr Erik Isokangas, for guiding me and constantly providing fresh insight throughout the course of the project.

Secondly, I would like to acknowledge Professor Chandima Ekanayake, my UQ academic supervisor, for taking the time to sit down with me and discuss complications I was having regarding my project in times of need.

Thirdly, I would like to thank Stuart Addinell from Mining3, and my fellow placement students: Paul Sachse, Alex Goodsell, and Shannon Law, for providing guidance and support throughout the difficult aspects of the project.

Lastly, I would like to acknowledge Christopher Leonardi and the EAIT Student Employability Team, for keeping me on track with all my assessment throughout the course of this placement, and teaching me about workplace communication and how to make a good impression when applying for jobs.

Contents

List of Figures **6**

List of Tables **7**

1 Introduction **9**
1.1 Context . . . 9
1.2 Aim . . . 11
1.3 Objectives . . . 11
1.4 Scope . . . 12
1.5 Deliverables . . . 12

2 Literature Review **14**
2.1 Wireless Power Transfer Systems . . . 14
2.1.1 Capacitive Wireless Power Transfer . . . 14
2.1.2 Inductive Wireless Power Transfer . . . 14
2.1.3 Capacitive WPT vs. Inductive WPT . . . 15
2.2 Resonant Inductive Wireless Power Transfer . . . 17
2.2.1 Primary Side Driver Circuit . . . 19
2.2.2 Transmitter and Receiver Circuits . . . 20
2.2.3 Secondary Side Rectifier Circuit . . . 20
2.3 Coil Performance . . . 21
2.3.1 Coupling Coefficient . . . 21
2.3.2 Coil Quality Factor . . . 22
2.3.3 Skin Depth and the Skin Effect . . . 23
2.3.4 Litz Wire . . . 24
2.3.5 Optimal Drive Current Frequency . . . 24
2.3.6 Magnetic and Metallic Shielding . . . 25
2.4 Dynamic Wireless Power Transfer System Design . . . 26
2.4.1 Horizontal and Movement Misalignment . . . 26
2.4.2 Segmentation . . . 28
2.5 Transmitter and Receiver Topologies . . . 29
2.5.1 Circular Pad Transmitter and Circular Pad Receiver . . . 29
2.5.2 DD Pad Transmitter and DD Pad Receiver . . . 30
2.5.3 DD Pad Transmitter and DDQ Pad Receiver . . . 30
2.5.4 Crossed DD Pad Transmitter and DD Pad Receiver . . . 32

3 Project Methodology **33**
3.1 Research Investigation . . . 33
3.2 ANSYS Simulations . . . 33
3.3 Small-Scale Resonant System Investigation . . . 35
3.4 Small-Scale Resonant System Tuning . . . 36
3.5 Automated Tuning for the Resonant System . . . 38

3.6 Segmentation Implementation 39

4 Results and Analysis **41**
4.1 Simulation Results 41
4.1.1 Rectangular Coil Width 41
4.1.2 Transmitter-Receiver Separation (Air Gap) 42
4.1.3 Horizontal Misalignment 42
4.2 Small-Scale Resonant System Results 44
4.2.1 Resonance Tuning Investigation 44
4.2.2 Automatic Resonance Tuning 47

5 Conclusions and Recommendations **48**

6 References **51**

7 Appendices **54**
Appendix A: Professional Development 54
Appendix B: Project Management 57
Appendix B.1: Project Timeline 57
Appendix B.2: Risk Management 60
Appendix B.3: Resource Requirements 62
Appendix B.4: Project Opportunities 63
Appendix C: Resonance Tuning Finite State Machine 64
Appendix D: Finite State Machine TIVA Code 65

List of Figures

1 Electric Vehicle Powering System Using Overhead Contacts [1] 10
2 Autonomous Electric Hauler Prototype 2018 11
3 Capacitive Wireless Power Transfer Circuit [2] 15
4 Inductive Wireless Power Transfer Circuit [3] 15
5 efficiency of inductive and capacitive WPT vs. air gap distance [4] . . . 17
6 Resonant Inductive Wireless Power Transfer Circuit [5] 18
7 Full System [6] 19
8 DC-AC Inverter Circuit (H-Bridge) [7] 20
9 The Four Compensator Circuit Topologies [3] 21
10 Full-Bridge Rectifier Circuit [3] 21
11 the current density throughout the cross-section of a wire/conductor when the skin effect is significant [8] 24
12 the constituents of Litz wire [9] 24
13 Magnetic and Metallic shielding using ferrite strips and a metal backplate 25

14 two charging pads (transmitter and receiver) with a horizontal offset between them [10] . . . 27
15 receiver pad moving along multiple transmitter pads [11] . . . 27
16 graph of the output power as the electric vehicle moves - two different TX-RX topologies investigated: DD to DD and "crossed DD" to DD [12] 28
17 The Online Electric Vehicle (OLEV) developed by KAIST [13] . . . 29
18 circular charging pad . . . 29
19 DD pad (on the left) and a crossed DD pad (on the right) [12] . . . 30
20 DDQ charging pad [10] . . . 31
21 the system which manages the induced voltage in a DDQ pad [10] . . . 31
22 crossed DD pad transmitter array with a DD pad receiver [12] . . . 32
23 ANSYS model of a DD pad transmitter and receiver . . . 34
24 magnetic field intensity heat map . . . 34
25 small-scale DD pad transmitter and receiver . . . 36
26 primary side setup used to drive the small-scale system . . . 36
27 the small-scale DD pads used for the resonance tuning investigation . . 37
28 automatic resonance tuning setup: current sensor, TIVA, op-amp, DC power supply . . . 38
29 integrated DD charging pads (large scale) with magnetometers for segmentation . . . 40
30 The Electric Vehicle . . . 40
31 graph displaying coupling coefficient vs width of rectangular coils . . . 41
32 coupling coefficient vs air gap distance for square coils with a 120mm side length . . . 42
33 DD charging pad with ferrite bars and steel back-plate . . . 43
34 coupling coefficient vs horizontal misalignment (DD to DD coupling) . 43
35 normalised output power vs. horizontal misalignment for a non-resonant-tuned system . . . 45
36 normalised output power vs. horizontal misalignment for a resonant-tuned system . . . 45
37 the factor of improvement introduced by resonance tuning vs. horizontal misalignment . . . 46
38 Graphical Representation of the Project Timeline (Gantt Chart) . . . 59

List of Tables

1 Capacitive WPT: strengths and weaknesses w.r.t electric vehicle charging 16
2 Inductive WPT: strengths and weaknesses w.r.t electric vehicle charging 16
3 Summary of Learning Events and EA Competencies Developed . . . 55
4 Project Timeline - First Half of Placement . . . 57
5 Project Timeline - Second Half of Placement . . . 58
6 Mining 3 Risk Assessment Matrix . . . 60

7 Risk Analysis 61
8 Necessary Resources for Project Completion 62

1 Introduction

1.1 Context

Migration towards electric vehicles has become a major focal point for mining research. Primarily, this is due to the issues and limitations associated with diesel powered vehicles [14]. Some of these include:

- Rising fuel prices.
- Ventilation requirements.
- Inefficiencies in diesel energy conversion.

Electric vehicles do not require ventilation, convert energy more efficiently, and are battery powered. Eliminating the requirement for ventilation is crucial, as it dictates a large portion of a mine's infrastructure, and contributes significantly to the energy usage within an underground mine [14]. Furthermore, implementing batteries not only mitigates the need for expensive diesel fuel, but improves low speed acceleration [14].

When integrating an electric vehicle into a mining environment, the method used to either charge the battery or electrically power the vehicle is a primary concern. Two existing methods include:

- Temporarily removing the electric vehicle from operation to replace the battery.
- An overhead catenary system using pantograph contacts to provide constant DC power [1].

Removing the electric vehicle from operation is the simplest method, however, is time consuming and requires additional personnel. Conversely, the overhead catenary system can provide much faster haul cycles, since the mining vehicle maintains electrical contact for its entire route, allowing the vehicle to receive constant power to the motorised wheels [1]. Figure 1 demonstrates how the mining vehicle maintains contact with the overhead power lines.

A major downside regarding the overhead catenary system is that the framework is fixed in place. Hence, if a haul route was to be changed, the entire overhead cable network would need to be re-routed. Therefore, it is not suitable for a mine with a fast-changing infrastructure.

To summarise, the limitations involved with existing electric vehicle systems in mining are:

- Haul cycle slowed down when the electric vehicle is removed from operation.

- Static framework preventing the changeability of haul routes.

Therefore, a charging system which can provide a solution for both of these existing limitations is required.

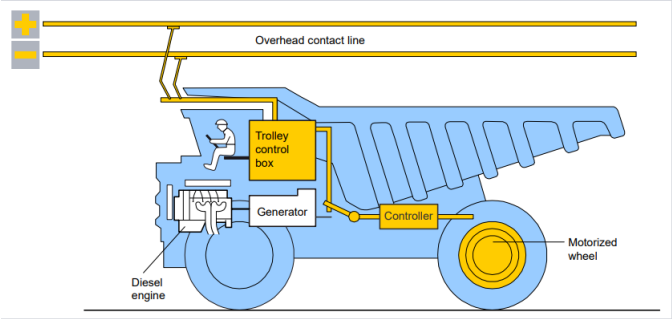

Figure 1: Electric Vehicle Powering System Using Overhead Contacts [1]

To counter the limitations discussed previously, a portable charging system which could wirelessly deliver power to the electric vehicle on-route could be implemented. This would allow the battery to be charged whilst the vehicle was in motion, i.e., dynamic wireless charging. The portability of the system would mitigate the issues involved with a static framework and the changing of haul routes. Additionally, the vehicle would no longer require temporary removal from the haul cycle to change batteries.

An electric vehicle which could wirelessly charge along its haul route would still require a driver. To eliminate this economic deficit, a self-navigation system could be implemented, deeming the electric vehicle completely autonomous. Also, by automating the electric vehicle, the safety hazard involved with the personnel required to operate the vehicle would be mitigated. In summary, if the mining vehicle was autonomous, and sufficient wireless power could be transferred dynamically during one route cycle, the vehicle could theoretically operate indefinitely without human interaction.

In 2018 (last year), five BE/ME UQ students worked together to develop the first prototype of an autonomous electric hauler with a portable wireless charging system. The prototype vehicle is depicted in Figure 2. The wireless charging component of the prototype was capable of dynamically powering LEDs through the coupling of two inductive coils, a transmitter (TX) coil and a receiver (RX) coil. The focus of this project is to develop a new wireless power transfer system which improves upon the previous design.

Figure 2: Autonomous Electric Hauler Prototype 2018

1.2 Aim

The aim of this project was to research, investigate, and propose designs for a dynamic wireless charging system which could be implemented to power an autonomous electric vehicle whilst in motion.

1.3 Objectives

The objectives of this project are:

- Develop an in-depth understanding of the subject matter relevant to this project, by researching and collating current state of the art systems for wireless charging.
- Relate the existing state of the art wireless charging systems to the specifications and requirements of this project. The wireless charging system is required to deliver power dynamically (not whilst the vehicle is stationary) and be portable.
- Propose designs based on the research and generate simulations to test them.
- Build small-scale prototypes for the designs which provided the best results in simulation.
- Assess the wireless charging capabilities of the small-scale prototypes in terms of important characteristics such as: efficiency, susceptibility to misalignments, transfer capabilities over different air gaps, etc.
- Integrate the final design with the rest of the systems involved with the prototype autonomous electric vehicle.
- Draw conclusions based on the research, simulations, and experiments conducted, and use these conclusions to advise future research and development for this project.

- Produce reports which deliver the findings of the project, provide insight into the investigation process, and reflect upon personal development as an engineer.

1.4 Scope

This project concerns the development of a dynamic wireless charging system for an autonomous electric hauler (electric mining vehicle). The project is comprised of numerous smaller tasks which all contribute to the system's overall functionality. These include:

- The collation of literature to determine the most effective wireless power transfer technology for dynamic wireless charging.
- The development of power electronics circuitry to drive the primary side of the system with high-power high-frequency AC.
- The simulation of different primary (TX) and secondary (RX) coil designs using ANSYS.
- The construction and testing of different TX and RX coil designs.
- The development of power electronics circuitry to rectify the AC voltage induced in the RX coil to DC.
- The design of a frequency adjusting feedback network to maintain resonance between the primary and secondary compensator circuits.
- The development of a mechanism to be embedded into the primary side of the system which can detect the presence of the hauler.
- The development of circuitry to switch the TX coils on and off.
- Following the workplace safety procedures when constructing the system.

1.5 Deliverables

1. **Literature Review**
   A literature review must be constructed which clearly outlines the area of investigation. This includes research relevant to the various aspects of the project as well as existing state of the art systems.

2. **Online Reflective Journals**
   Five monthly journals must be submitted over the course of the six month placement. Each journal must describe professional development specifically related to the Engineers Australia Stage 1 Competencies.

3. **Project Proposal**
   A project proposal must be submitted which delivers the context of the project and describes the expected outcomes. The proposal must also outline the potential risks involved with any testing/construction.

4. **Interim Report**
   The purpose of the interim report is to compare the current progress of the project with the project plan presented in the proposal. Any results which have been collected should be presented.

5. **Oral Presentation**
   An oral presentation must be presented to peers as well as academic staff members. Also, prior to the assessed presentation, a presentation will be given at one of the Mining3 learning lunches.

6. **Final Report**
   This is the thesis which must be submitted at the end of the six month placement. It will document the progress and outcomes of the entire project.

7. **Mutual coupling and magnetic field simulations**
   In order to determine the optimal geometry/arrangement for the primary and secondary side of the induction system, simulations will be run using ANSYS Electronics Desktop. The simulations will concern the mutual coupling between the primary and secondary coils, as well as magnetic field heat maps for visualisation.

8. **Wireless power transfer system prototypes**
   Build prototype designs to investigate the conclusions drawn from the conducted research and the simulation data generated.

9. **Mining3 Presentation**
   On the last day of the 120 day placement, all the students will present their project findings to the rest of the employees at Mining3 at a learning lunch.

2 Literature Review

2.1 Wireless Power Transfer Systems

A wireless power transfer (WPT) system involves the transmission of electrical power without the use of wires or any type of physical link [15]. Instead, the system transfers electrical power by utilizing the properties of electromagnetic fields. WPT systems which operate over short distances (typically less than 1 metre), for example, wireless charging pads for cars, transfer electrical power using either magnetic or electrostatic induction [16][17]. Conversely, long distance WPT systems (potentially thousands of kilometres), for example, solar power satellites, transfer power using radio frequency electromagnetic radiation [18]. Regardless of how the power is transferred, and over what distance, all WPT systems consist of a primary (transmitter) side and a secondary (receiver) side. The electrical power is transmitted from the primary (TX) side, and is then received by the secondary (RX) side.

This project is focused on the development of a wireless charging system for an autonomous electric mining vehicle. Therefore, the system is required to transfer power over a short distance (less than 1 metre). As discussed previously, a WPT system which transfers power over a short distance must utilize either inductive or capacitive coupling. There are numerous existing methods for short range wireless power transfer, all with different advantages and disadvantages depending on the specific application. The most popular of these methods include: Capacitive, Inductive, and Resonant Inductive wireless power transfer [3].

2.1.1 Capacitive Wireless Power Transfer

Typically, capacitive WPT systems utilize two pairs of conductive metal plates, as depicted in figure 3. When an AC voltage is applied to the primary side, two coupled capacitors are formed, establishing a closed circuit [2]. Figure 3 shows that the electric fields generated by each of the two coupling capacitors have opposite polarities. This demonstrates that current flows from primary to secondary through one capacitor, and from secondary to primary through the other [2]. This is what establishes the closed circuit, allowing power to flow from the primary side to the secondary side, whilst also providing a return path for the current [16].

2.1.2 Inductive Wireless Power Transfer

Figure 4 contains a circuit diagram for a system utilizing inductive wireless power transfer technology. There is a primary transmitter coil (TX coil) connected to a driver circuit, and a secondary receiver coil (RX coil) connected to a full-bridge rectifier circuit [3]. The driver circuit excites the RX coil with a sinusoidal current. This changing current in the TX coil induces a voltage in the RX coil. This process is

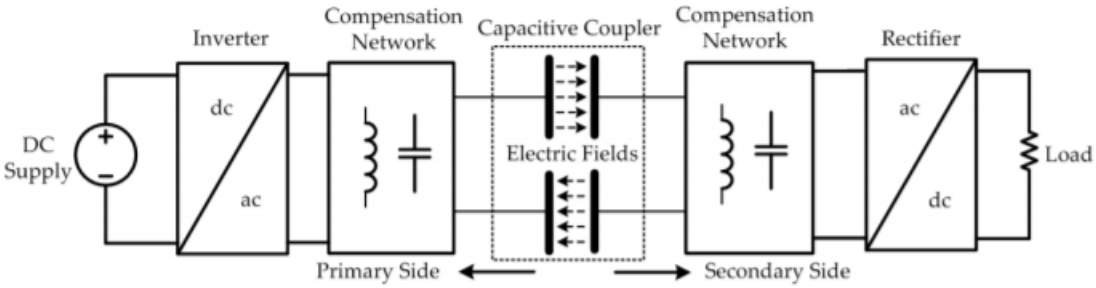

Figure 3: Capacitive Wireless Power Transfer Circuit [2]

called electromagnetic induction [3]. The induced voltage in the RX coil is then rectified to DC and used to drive the load. The TX and RX coil are not connected, hence, by electromagnetic induction, the power is transferred wirelessly from the driver circuit to the load.

The efficiency of the inductive power transfer is largely determined by two main factors regarding the TX and RX coils. The first is the individual quality of both the coils, and the second is the coupling coefficient between the coils. This is discussed in more depth further on in the "Coil Performance" section, along with methods for improving both these factors.

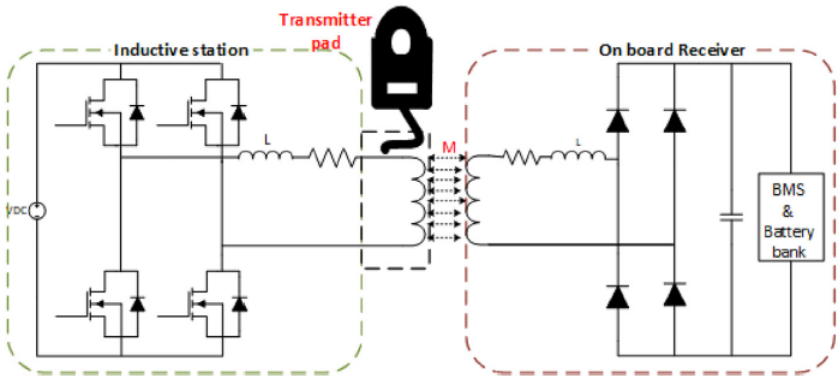

Figure 4: Inductive Wireless Power Transfer Circuit [3]

2.1.3 Capacitive WPT vs. Inductive WPT

To critically determine the most suitable wireless power transfer method for this project, the strengths and weaknesses of each method must be assessed in the context of dynamic electric vehicle charging. Tables 1 and 2 summarise the strengths and weaknesses of capacitive and inductive WPT respectively.

Capacitive WPT (Dynamic Electric Vehicle Charging)	
Strengths	**Weaknesses**
• Does not require magnetic shielding to achieve high efficiencies. This eliminates the requirement for expensive ferrites [2]. • High efficiencies can be achieved at very high frequencies (MHz range) [2].	• The power transfer distance of capacitive WPT is much smaller than that of inductive WPT [4]. Figure 5 demonstrates this graphically. • Parasitic capacitances can potentially cause significant inefficiencies in the system, as a result of cross-coupling between the capacitor plates and the vehicle chassis [2]. • The system is not robust to misalignments between capacitor plates [4].

Table 1: Capacitive WPT: strengths and weaknesses w.r.t electric vehicle charging

Inductive WPT (Dynamic Electric Vehicle Charging)	
Strengths	**Weaknesses**
• Can maintain high efficiencies over large air gaps unlike capacitive WPT [4]. Again, figure 5 demonstrates this. • The system can run efficiently at a broad range of frequencies (10's kHz to 10's MHz) [4]. • TX and RX coil can still inductively couple under misalignment, and a proportional amount of efficiency can be maintained.	• Due to any metal present near the system, for example, the vehicle chassis, eddy current losses will occur [4]. • Magnetic flux density at a distance "r" from the TX coil drops of with a $1/r^3$ relationship.

Table 2: Inductive WPT: strengths and weaknesses w.r.t electric vehicle charging

To determine which method is more applicable (IWPT or CWPT), we must consider the requirements for this electric mining vehicle charging system. The air gap be-

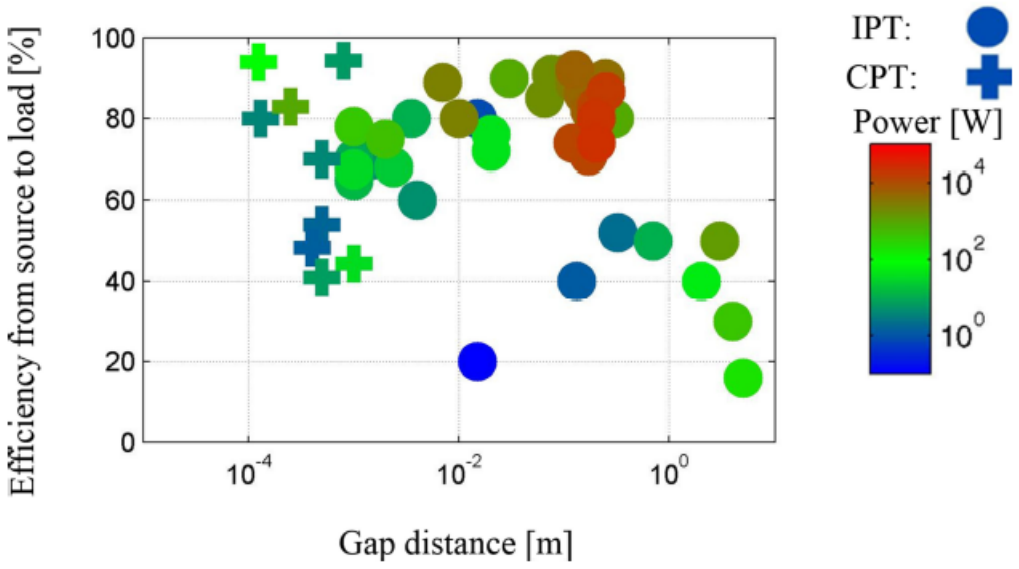

Figure 5: efficiency of inductive and capacitive WPT vs. air gap distance [4]

tween the receiver circuit on the vehicle, and the transmitter circuit on the ground, will be at minimum, approximately 10cm. As mentioned in tables 1 and 2, IWPT can maintain higher efficiencies with larger air gaps than CWPT. Additionally, there will often be misalignments between the vehicle and the charging system, since the vehicle will be charging dynamically. Table 1 mentions that CWPT is not robust to misalignments (IWPT can maintain more efficiency under misalignment), hence, would not be effective for dynamic vehicle charging. In conclusion, an inductive WPT system would be more effective for dynamically charging an electric mining vehicle.

Although inductive WPT is a more applicable technology for this project than capacitive WPT, inductive WPT still has weaknesses. Table 2 mentions the $1/r^3$ drop-off in magnetic flux density generated by the TX coil. This is where a technology called resonant inductive WPT improves upon the existing inductive WPT.

2.2 Resonant Inductive Wireless Power Transfer

The current state of the art technology for wireless power transfer is the resonant inductive wireless power transfer system, displayed in figure 6. A resonant inductive WPT system consists of an LC resonator circuit on both the primary and secondary side of the system, as demonstrated in figure 6. The RX and TX coils are the inductors for the LC resonators, and both coils are then matched with a capacitor. The primary and secondary LC circuits need to have the same resonant frequency, otherwise they cannot resonate simultaneously. The resonant frequency of an LC circuit

can be calculated using equation 1 [5].

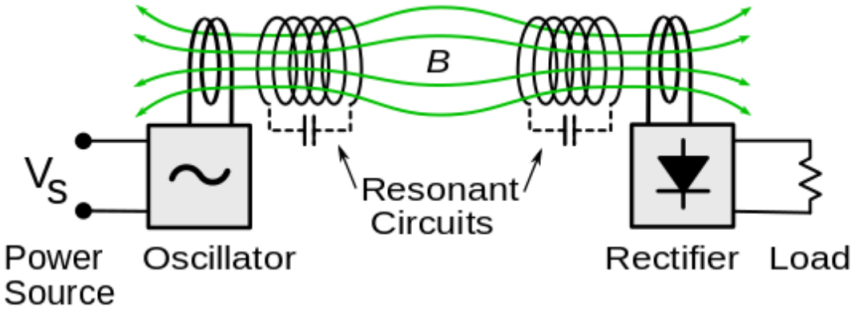

Figure 6: Resonant Inductive Wireless Power Transfer Circuit [5]

$$f = \frac{1}{2\pi\sqrt{LC}} \tag{1}$$

If the primary and secondary LC circuits have the same resonant frequency, and the system is driven at this resonant frequency, the strong coupling which occurs between resonant coils can be taken advantage of [5]. Resonant coils can achieve strong coupling even over air gaps which are several times the diameter of the coils [5]. This is because only a small percentage of the primary coil's field needs to couple with the receiver coil, in order to build up an intense field which oscillates at the resonant frequency. This oscillating magnetic field then tunnels energy from primary to secondary, instead of the energy diverging in all directions from the primary, as with normal inductive WPT. This is why resonant inductive WPT is much more effective for developing strong coupling over large air gaps than inductive WPT.

Strong coupling over a significant air gap (tens of centimetres wide for most vehicles) is an important trait to consider when investigating the wireless charging of an electric mining vehicle. This is due to a mining vehicle's requirement for bottom clearance, as vehicle routes are rarely perfectly flat roads. In conclusion, resonant inductive WPT is the most effective technology for this project.

Figure 7 depicts a full resonant inductive WPT system, which is setup to wirelessly charge a battery. The main components of the system are:

1. High frequency DC-AC inverter (section 2.2.1).
2. Primary and Secondary Compensator Circuits (resonators) (section 2.2.2).
3. High frequency AC-DC rectifier (section 2.2.3).

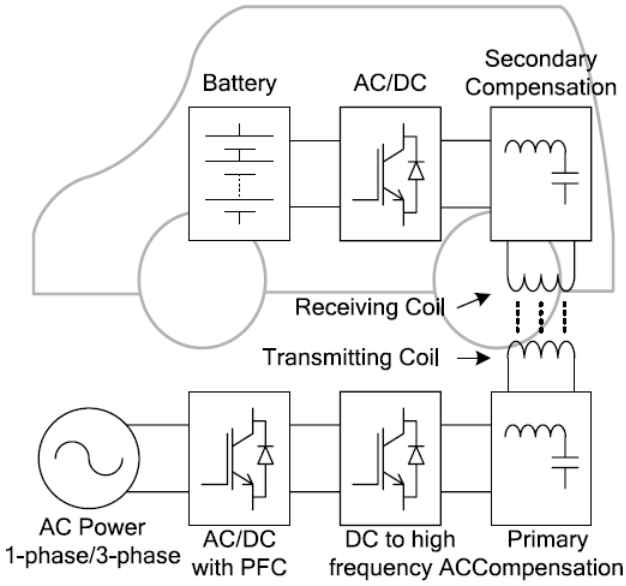

Figure 7: Full System [6]

2.2.1 Primary Side Driver Circuit

The resonant inductive WPT system is required to wirelessly transfer 1kW of power from the primary side to the secondary side. Therefore, the square wave which is used to drive the primary side of the system at the resonant frequency must be high-power (1kW). A circuit called a DC-AC inverter can generate a high-power square wave using a DC power supply, a micro-controller, gate drivers, and a H-bridge.

Figure 8 shows how the DC power supply and the load are connected to the H-bridge in the DC-AC inverter circuit. The load in this scenario is the primary side of the resonant inductive WPT system. The four MOSFETS in the H-bridge (figure 8) are switched on and off by TTL signals. The first TTL signal controls S_1 and S_4, and the second TTL signal which is 180^o out of phase (inverted) controls S_2 and S_3 [7].

The two TTL signals are generated by a micro-controller, however, micro-controllers cannot output the required current to switch MOSFETS fast and efficiently. Therefore, the two TTL signals from the micro-controller are input into gate driver circuits which are then connected to the MOSFETS [7].

If the frequency of the high-power square wave generated by the DC-AC inverter is equal to the resonant frequency of the system, the square wave harmonics will be filtered out. Therefore, the voltage and current waveforms in the TX and RX coils will be a sinusoid at the resonant frequency. The frequency of the TTL waves output by the micro-controller can be adjusted until the resonant frequency of the resonant in-

ductive WPT system is found.

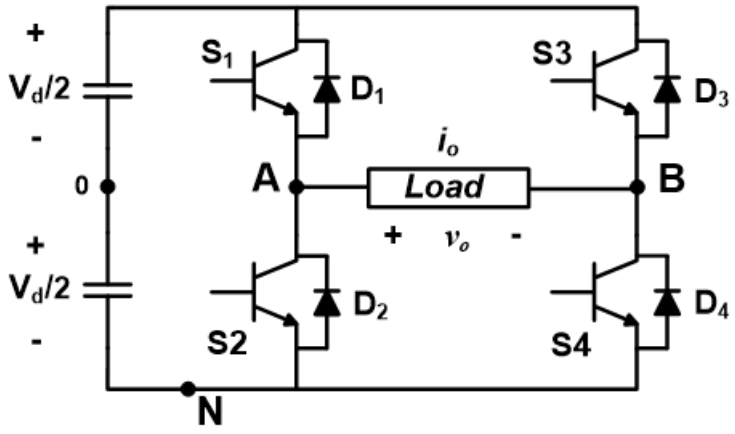

Figure 8: DC-AC Inverter Circuit (H-Bridge) [7]

2.2.2 Transmitter and Receiver Circuits

With a resonant inductive power transfer system, the capacitors and inductors which form the primary and secondary side LC resonators, are called compensator circuits (the inductors for the LC resonators being the coils). The inductor and capacitor in the compensator circuit can be connected in either series or parallel. This provides four unique topologies: series-series (SS), series-parallel (SP), parallel-series (PS), and parallel-parallel (PP), as shown in figure 9 [3].

The series-series compensator circuit topology is the most effective for electric vehicle charging. There are two main reasons for this. Reason 1: the resonant frequency of the transmitter and receiver resonant circuits is not affected by the load or the mutual inductance of the TX and RX coils [3]. This is beneficial for a dynamic wireless charging system, since these parameters change as the electric vehicle moves across the charging pad. Reason 2: the series-series topology ensures that the system maintains a unity power factor, hence, a higher efficiency can be achieved [3]. A minor downside to this topology, however, is that the efficiency of the system is highly frequency dependent [5]. To combat this, a frequency tuning feedback network can be built into the system, which maintains resonance between the primary and secondary compensator circuits by adjusting the drive frequency accordingly. This is discussed in more depth further on in the "resonance feedback network" section.

2.2.3 Secondary Side Rectifier Circuit

The secondary side circuit must utilize the transferred power to charge the battery of the electric vehicle. The voltage induced in the secondary side coil is a high frequency

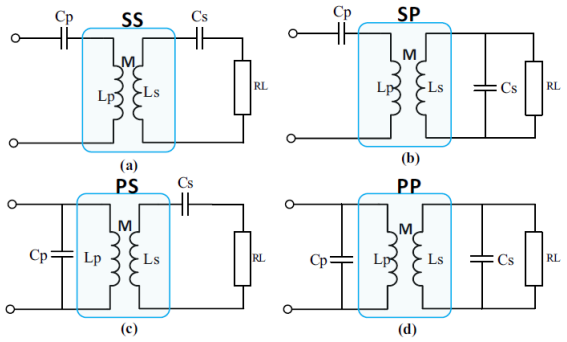

Figure 9: The Four Compensator Circuit Topologies [3]

AC voltage, however, a DC voltage is required to charge the battery. Therefore, a full-bridge rectifier circuit (figure 10) must be implemented on the secondary side to convert the AC induced voltage to DC. This DC voltage then becomes the input for the battery charging circuit.

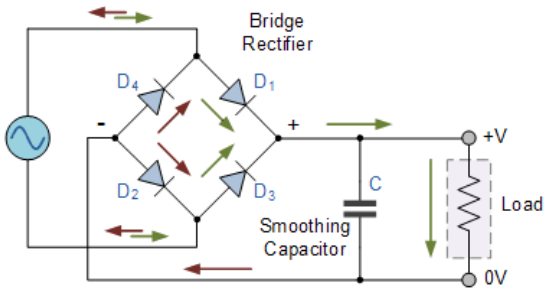

Figure 10: Full-Bridge Rectifier Circuit [3]

2.3 Coil Performance

A wireless charging system which utilizes resonant inductive WPT technology can achieve high efficiencies due to the strong coupling which occurs between resonant coils. However, if the TX and RX coils are not initially designed for optimal performance, the efficiency of the system will be inhibited. Hence, the following section explores methods and concepts which can be used to improve/optimise coil performance.

2.3.1 Coupling Coefficient

A resonant inductive WPT system consists of a primary transmitter coil (TX coil), and a secondary receiver coil (RX coil), separated by an air gap. When AC current flows through the TX coil, a changing magnetic flux is produced. This changing magnetic flux induces an AC voltage in the RX coil. If a load is attached to the RX coil,

an AC current will flow, hence, power has been transferred between the coils wirelessly. A transformer transfers power using this same concept, however, the primary and secondary coils of a transformer are wound around a common magnetic core [19]. The flux produced by the primary coil of the transformer flows through the magnetic core and then couples with the secondary coil, hence, there is very little flux leakage [19]. Since resonant inductive WPT involves inductive coupling over an air gap, the flux leakage is much more significant. Hence, the efficiency of the power transfer in a resonant inductive WPT system is less than that of the power transfer in a transformer.

A concept called the **coupling coefficient** is very important when modelling a resonant inductive WPT system, as it indicates the degree of flux leakage, which has a direct impact on the efficiency of the system. When the TX and RX coils inductively couple, ideally, all the magnetic flux produced by the TX coil will link with the RX coil, deeming the coils perfectly coupled, with a coupling coefficient of 1 (k=1). Conversely, if the coupling coefficient is 0 (k=0), no flux links with the RX coil, hence there is 100% flux leakage, and the coils are considered magnetically isolated. However, in practice, there is always some degree of flux leakage.

The coupling coefficient, k, represents the fraction of flux leakage between the TX and RX coils. If $k > 0.5$, the coils are tightly coupled, and if $k < 0.5$, the coils are loosely coupled. Now, the larger the flux leakage, the more inefficient the wireless power transfer becomes [5]. Hence, when designing the TX and RX coils for the resonant inductive WPT system, their coupling coefficient must be maximized, to improve the power transfer efficiency.

The coupling coefficient between the primary and secondary coils can be determined from equation 2 [20].

$$k = \frac{M}{\sqrt{L_{TX} L_{RX}}} \tag{2}$$

L_{TX} is the self-inductance of the TX coil, L_{RX} is the self-inductance of the RX coil, and M is the mutual inductance between the coils. Equation 2 shows that with a higher mutual inductance, and reduced self-inductances, an increased coupling coefficient can be achieved [20].

2.3.2 Coil Quality Factor

A coil can be modeled by an inductance, L, and a series resistance, R. The series resistance dissipates reactive energy, reducing the efficiency of the coil. The quality factor (Q factor) of a coil is the ratio between the reactance of the coil, and the resistance, as shown in equation 3 [21].

$$Q = \frac{X_L}{R} \tag{3}$$

$$X_L = \omega L \tag{4}$$

The higher the Q factor, the more efficient the coil. To increase the Q factor, the coil reactance must be maximized, and the resistance must be minimized. The coil reactance can be increased by either increasing the frequency of the AC driving current, or the inductance of the coil. This can be deduced from equation 4. Methods for increasing the coil inductance and drive current frequency whilst maintaining a low resistance are discussed further on.

2.3.3 Skin Depth and the Skin Effect

A quantity called the skin depth can be used to model the current density throughout the cross section of a wire. The skin depth can be calculated from equation 5 [8].

$$\delta = \sqrt{\frac{2\rho}{\omega\mu}} \tag{5}$$

ρ is the electrical resistivity of the wire, μ is the magnetic permeability of the wire, and ω is the angular frequency of the current. Equation 5 demonstrates that the skin depth is smaller for larger frequencies [8]. This is an important concept.

Since the relationship between skin depth and frequency is now understood, if the relationship between skin depth and current density is considered, it can be utilized to understand the relationship between frequency and current density. If J_s is the current density at the surface of the wire, d is the depth beneath the surface of the wire, and δ is the skin depth, then the current density at any depth can be described by equation 6 [8].

$$J = J_s e^{-\frac{d}{\delta}} \tag{6}$$

Equation 6 demonstrates that the current density reduces exponentially as the depth increases. When the depth is equal to the skin depth, the current density is only 37% than that of the surface current density, J_s. Therefore, when the skin depth is small w.r.t. the radius of the wire, it can be deduced that most of the current will flow through the outer rim of the wire. When this occurs, the effective resistance of the wire is increased, since the current is now constrained to a smaller cross-sectional area [8]. **This is known as the skin effect**. Figure 11 demonstrates the skin effect visually.

It was deduced previously that the skin depth was smaller at higher frequencies. Therefore, it can be deduced that the **skin effect** becomes **more significant** at **higher**

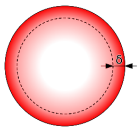

Figure 11: the current density throughout the cross-section of a wire/conductor when the skin effect is significant [8]

frequencies. Hence, it is very important to determine methods for reducing the skin effect when high frequency AC current is present.

2.3.4 Litz Wire

Litz wire is made up of multiple strands of individually insulated copper wire, shown in figure 12.

Figure 12: the constituents of Litz wire [9]

When the skin depth becomes much smaller than the radius of single strand copper wire, due to high AC current frequencies, the skin effect becomes significant and the resistance of the wire increases, as discussed previously. Litz wire, however, consists of multiple copper strands of a very small radius. Therefore, if compared at the same frequency as the single strand wire, the skin depth is now larger w.r.t. the radius of the individual Litz wire strands, and the skin effect is reduced [22].

2.3.5 Optimal Drive Current Frequency

In a resonant inductive WPT system, the TX coil must be driven by an AC current. This changing AC current in the TX coil induces a voltage in the RX coil, allowing power to be transferred wirelessly. If a DC current is used, no voltage will be induced in the RX coil, hence no power will be transferred.

The choice of frequency for the AC drive current is very important. As discussed previously, to increase the Q factor of a coil, the frequency of the AC current can be increased. However, it was also previously discussed that by increasing this frequency, the resistance of the coil will increase, due to the skin effect. This increased resistance will reduce the Q factor of the coil. To minimize the increased resistance due to the skin effect, the coil can be constructed from Litz wire, as discussed previously.

In summary, increasing the frequency of the AC current both increases and decreases

the Q factor. Hence, naturally, there must exist a frequency which optimizes the Q factor of the coils. This is the optimal drive current frequency and can be determined through experimentation. If the coils are constructed from Litz wire, a much higher optimal Q factor can be achieved, allowing for better system efficiency.

2.3.6 Magnetic and Metallic Shielding

Shielding can be used to improve the coupling between the transmitter and receiver coils in a resonant inductive WPT system. It involves placing ferrite strips and a sheet of either aluminium or steel under both the transmitter and receiver coils, as demonstrated in figure 13.

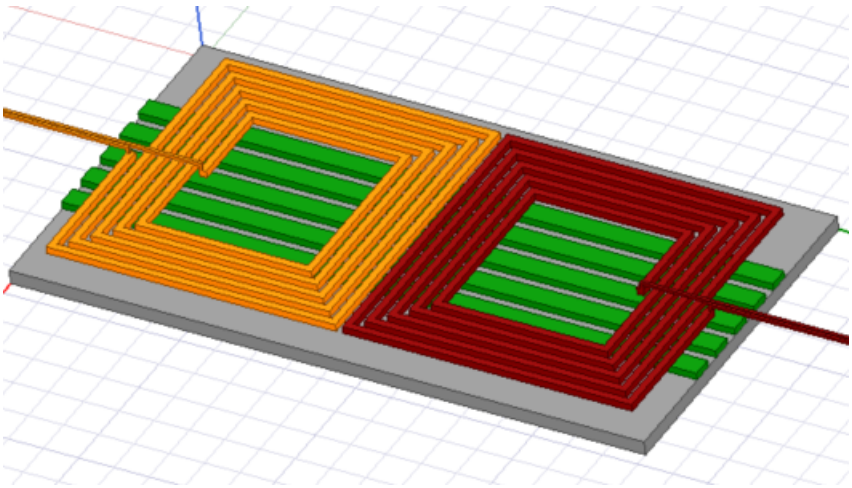

Figure 13: Magnetic and Metallic shielding using ferrite strips and a metal back-plate

Ferrite strips, which have a high magnetic permeability, are placed underneath the coils (figure 13), redirecting the leakage flux to travel from the transmitter coil to the receiver coil, and vice versa [13]. As a result, there is less leakage flux, improving the coupling between the coils. The ferrite strips also improve the mutual inductance between the coils, and the self inductance of each coil [13]. This use of ferrite to improve inductive coupling is called **magnetic shielding**.

When a metal sheet is placed underneath a coil excited with AC current, due to Faraday's law of induction, the magnetic field produced by the coil induces electrical currents in the metal (eddy currents) [3]. These induced eddy currents produce their own magnetic fields, which cancel out the incident magnetic fields on the surface of the metal. Hence, the metal sheet can be used to reduce leakage flux [3]. This is called **metallic shielding**.

If the transmitter and receiver coils both use metallic shielding (metal plates) without any magnetic shielding (ferrite bars), the self-inductance of both coils will reduce,

as will the mutual inductance between the coils, despite the reduction in leakage flux [13]. However, if ferrite bars are placed between the coils and the metal plates, as shown in figure 13, the benefits of both the magnetic and metallic shielding can be preserved [13]. Another important concept is that the metal plate used for the metallic shielding must be thicker than the skin depth [13]. Hence, the frequency of operation for the inductive WPT system must be known before the metallic shielding is implemented.

2.4 Dynamic Wireless Power Transfer System Design

When designing a "static" wireless charging system, there are two main aspects which impact the overall performance of the system. These are:

1. The system's ability to minimise the reduction in power transfer as the air gap between the transmitter and receiver increases.

2. The system's ability to maintain a high efficiency as the air gap between the transmitter and receiver increases.

Alternatively, when designing a "dynamic" wireless charging system for an electric vehicle, more aspects are introduced which impact the overall performance of the system. These include:

1. The system's susceptibility to horizontal misalignment (section 2.4.1).

2. The system's susceptibility to movement misalignment (section 2.4.1).

3. Accurate timing within the system; the charging pads must only be active when the vehicle is in close proximity. This is defined as segmentation (section 2.4.2).

2.4.1 Horizontal and Movement Misalignment

Horizontal misalignment is present when the receiver pad on the vehicle is not perfectly aligned with the transmitter pad on the ground. The horizontal axis is the x axis, as depicted in figure 14. The horizontal misalignment is quantified by the size of the horizontal offset between the receiver pad on the electric vehicle, and the transmitter pad on the ground, demonstrated in figure 14 [23].

Susceptibility to horizontal misalignment concerns the WPT system's ability to maintain a significant power transfer when horizontal misalignment exists. For a dynamic WPT system, the electric vehicle is receiving wireless power whilst in motion, hence, perfect alignment is very difficult to maintain. Therefore, horizontal misalignment is very common. As a result, one of the key considerations when designing a dynamic

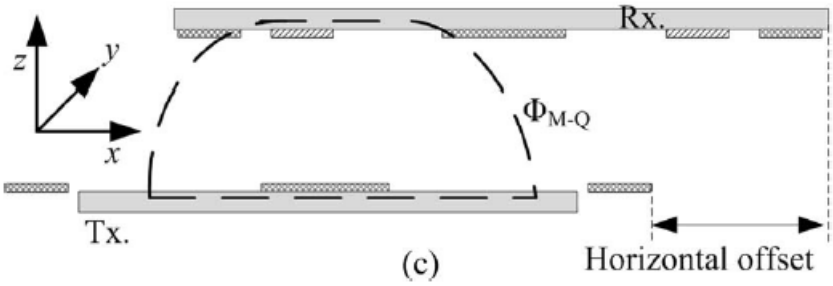

Figure 14: two charging pads (transmitter and receiver) with a horizontal offset between them [10]

WPT system is to minimise the decrease in transferred power when horizontal misalignment is present.

Movement misalignment is misalignment in the direction of the vehicle's movement, which is depicted as the y axis in figure 14. As the electric vehicle drives over the transmitter pads, the percentage of movement misalignment between the transmitter and receiver is constantly changing [23]. Figure 15 shows a receiver pad moving over two transmitter pads, allowing this movement misalignment to be visualised. At some instances, the electric vehicle's receiver pad will be perfectly aligned (on the y axis) with one of the transmitter pads on the ground. At this instance there would be 0% movement misalignment. At other instances, the receiver pad could be aligned half-way between two transmitter pads, hence, two 50% misalignments.

Movement misalignment in a dynamic WPT system is inevitable. Hence, another key consideration when designing a dynamic WPT system is to keep the transferred power as constant as possible as the movement misalignment varies. Figure 16 shows a graph of the output power vs movement misalignment (electric vehicle movement) for two different transmitter-receiver topologies. It is clear that the red output power curve has much less variation than the black output power curve. Therefore, the topology which produced the red output curve is less susceptible to movement misalignment, hence, would be more effective for a dynamic WPT system.

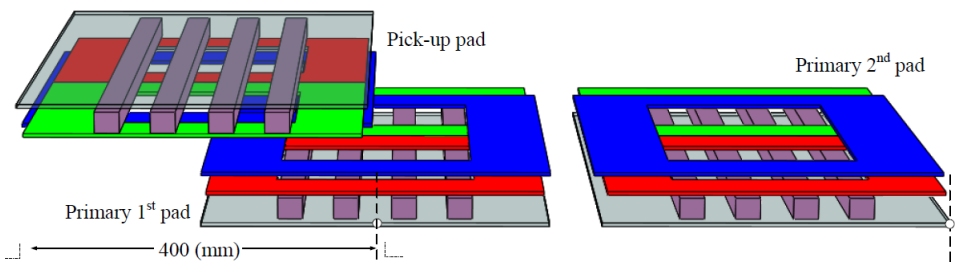

Figure 15: receiver pad moving along multiple transmitter pads [11]

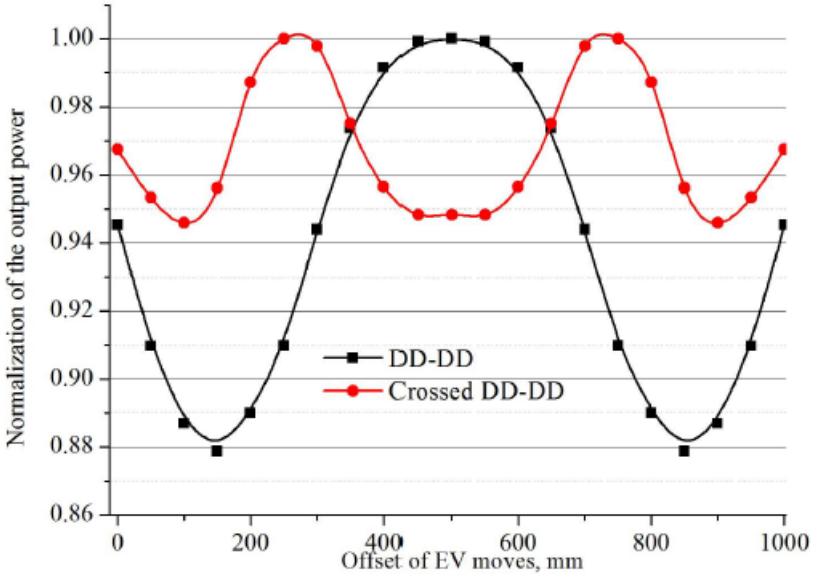

Figure 16: graph of the output power as the electric vehicle moves - two different TX-RX topologies investigated: DD to DD and "crossed DD" to DD [12]

2.4.2 Segmentation

Figure 17 displays the Online Electric Vehicle (OLEV), which was developed by KAIST (Korea Advanced Institute of Science and Technology). It is an electric bus which receives wireless power from electrical cables embedded in the surface of the road [24]. Only 5-15% of the entire road the bus operates on contains electrical cable for wireless charging [24]. The charging sections are placed at intervals along the bus route [24]. To ensure that each charging section is only active when the electric bus is approaching, the OLEV system uses segmentation [24].

Segmentation involves using a detection system to turn the charging sections on when the electric vehicle is approaching, and off once the electric vehicle leaves [24]. A system such as this ensures that no power is lost when the individual charging sections are not wirelessly transferring power to the electric vehicle. If the wires have current flowing though them, but no vehicle is present, the resistance in the wires will unnecessarily dissipate power and reduce efficiency.

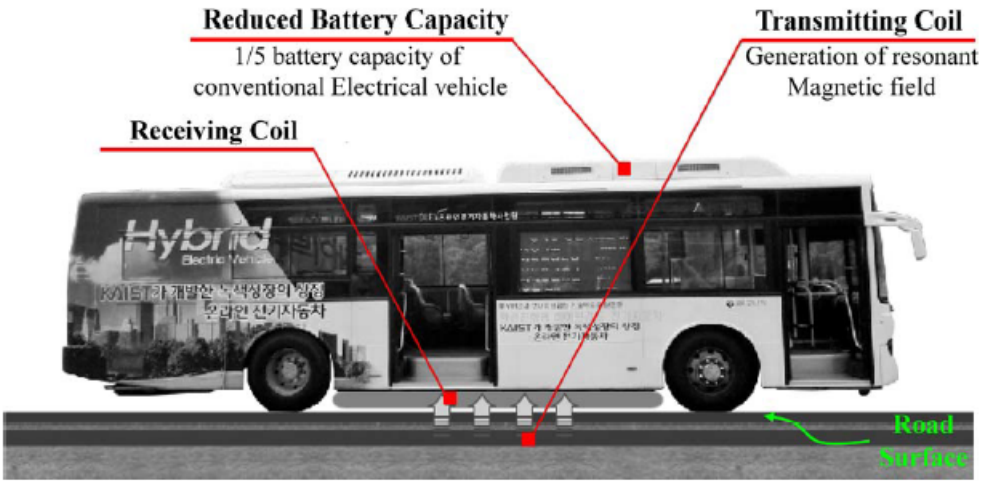

Figure 17: The Online Electric Vehicle (OLEV) developed by KAIST [13]

2.5 Transmitter and Receiver Topologies

This section discusses the advantages and disadvantages of some different transmitter-receiver topologies. The primary focus is the performance of each topology specific to a dynamic wireless charging system.

2.5.1 Circular Pad Transmitter and Circular Pad Receiver

Figure 18 shows a circular charging pad. This topology uses the circular charging pad as both the transmitter and receiver.

Figure 18: circular charging pad

Advantages:

- Simple design, easy to construct.
- Strong coupling over small air gaps without misalignment [10].

Disadvantages:

- The flux patterns of circular pads limit their ability to couple over larger air gaps [10].
- Flux patterns also reduce tolerance to horizontal misalignment [10].

2.5.2 DD Pad Transmitter and DD Pad Receiver

In figure 19, the charging pad on the left is a DD charging pad. This topology uses the DD charging pad as both the transmitter and receiver.

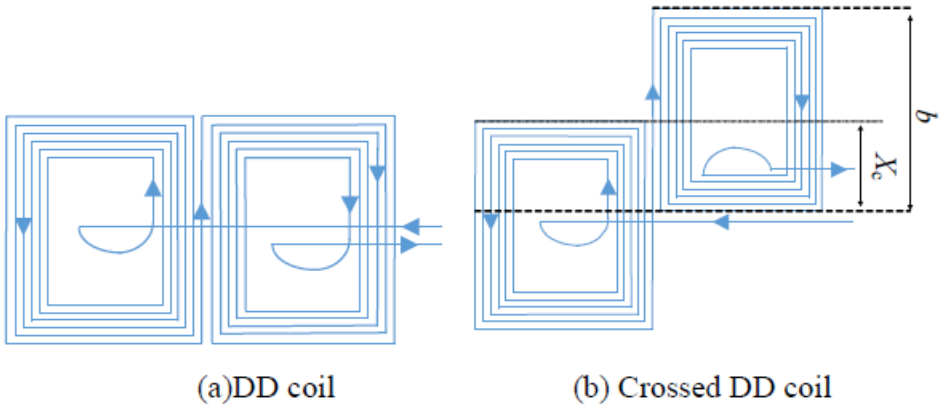

Figure 19: DD pad (on the left) and a crossed DD pad (on the right) [12]

Advantages:

- The overall charging zone of a DD pad (area on the x-y misalignment plane) is 5 times that of a circular pad, when constructed with the same materials [10].

Disadvantages:

- When the coupling of DD pads is tested under horizontal misalignment, dead zones occur [23]. These are zones where flux cancellation reduces the strength of the coupling [23].

2.5.3 DD Pad Transmitter and DDQ Pad Receiver

Figure 20 shows a DDQ charging pad. It is very similar to the standard DD pad, however, there is a quadrature coil integrated in as well, as depicted in figure 20. The quadrature coil is wound separately, and is positioned so as to fill the empty space present in the DD pad. This topology utilizes a DD pad as the transmitter, and a DDQ pad as the receiver.

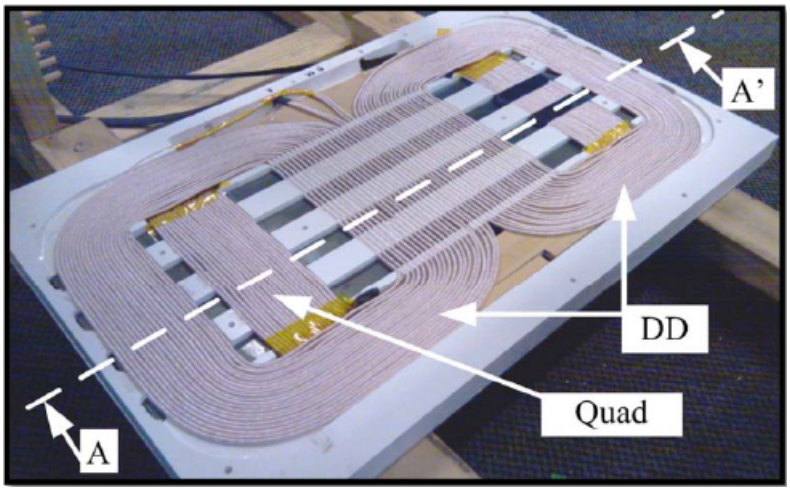

Figure 20: DDQ charging pad [10]

Advantages:

- The addition of the quadrature coil assists in the removal of the dead zones present in the previous DD to DD topology [11].
- Resultantly, the addition of the quadrature coil improves the system's robustness to horizontal misalignment [11].

Disadvantages:

- As mentioned previously, the quadrature coil in a DDQ pad is wound separately. Therefore, a separate compensator circuit and rectifier is required for the quadrature coil, as depicted in figure 21.
- Resultantly, managing the power transferred to a DDQ pad requires more complicated circuitry than a DD or circular pad. Again, this complicated circuitry is depicted in figure 21.

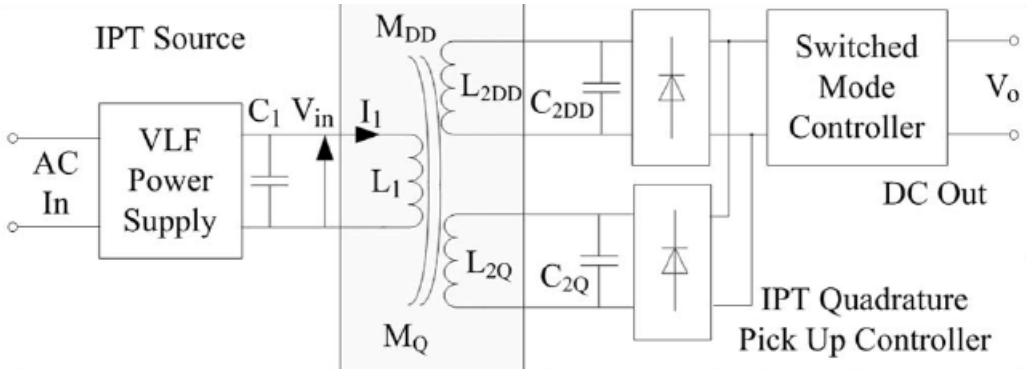

Figure 21: the system which manages the induced voltage in a DDQ pad [10]

2.5.4 Crossed DD Pad Transmitter and DD Pad Receiver

In figure 19, the charging pad on the right is a crossed DD pad. In a crossed DD pad, the two D shaped coils are offset by some select percentage. Figure 21 shows an array of crossed DD transmitter pads all offset by 50%. This topology uses the crossed DD pad as the transmitter and a DD pad as the receiver.

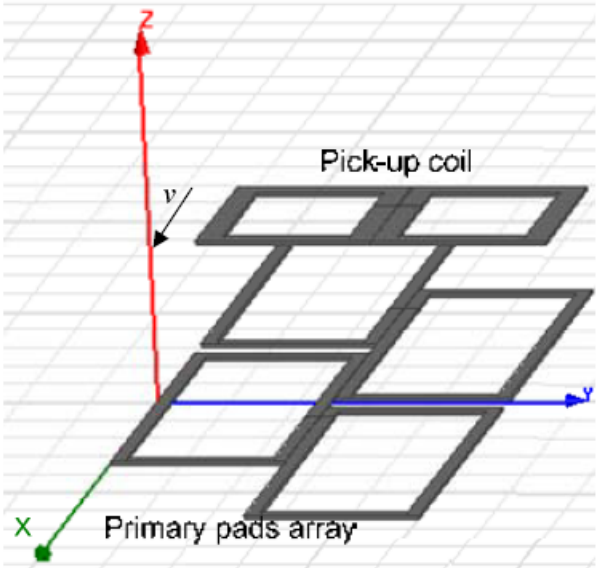

Figure 22: crossed DD pad transmitter array with a DD pad receiver [12]

Figure 16 is a graph of the normalised output power vs. movement misalignment, for both a "crossed DD to DD" topology, and a "DD to DD" topology. It can be clearly seen that the output power remains more constant for the "crossed DD to DD" topology.

Advantages:

- This topology is the most robust to movement misalignment [12]. This is a very important characteristic when considering a dynamic wireless charging system.
- Since this topology is robust to movement misalignment, the process of managing the transferred power to charge the vehicle battery is less demanding.

Disadvantages:

- Crossed DD transmitter pad arrays (figure 22) can be difficult to construct. This is because if the DD pads are not wound correctly, there can be significant flux cancellation within the transmitter array alone (the cancellation is not as a result of the receiver pad in any way).

3 Project Methodology

3.1 Research Investigation

The objective of the research phase was to deduce the most effective system topology for dynamic wireless power transfer.

Technical Approach:

1. A literature review was performed which involved researching state-of-the-art systems for dynamic wireless power transfer. Google Scholar was used to investigate the relevant IEEE articles.

2. The performance and characteristics of each system topology in the context of dynamic wireless power transfer was critically analysed.

3.2 ANSYS Simulations

The objective with ANSYS was to simulate the inductive coupling of different primary and secondary coil designs, whilst parametrising variables of interest (air gap, horizontal and movement misalignment, etc).

Technical Approach:

1. ANSYS Electronics Desktop was used to construct models for different transmitter and receiver coil designs. Figure 23 depicts the ANSYS model of a design with a DD pad transmitter and a DD pad receiver.

2. When constructing the coil models, variables of interest such as: coil length, coil width, air gap, and horizontal and movement misalignment were parametrised.

3. Simulations which generated magnetic field intensity heat maps in critical regions between the transmitter and receiver coils were initially run. These visual results assisted in providing an understanding of how the magnetic field changes when the relative positioning of the transmitter and receiver vary. Figure 24 shows a magnetic field intensity heat map positioned between two transmitter coils and one receiver coil.

4. ANSYS's sweep mechanism was applied to the aforementioned parametrised variables, the simulations were run, and magnetostatic reports were generated. The reports consisted of data tables which demonstrated how each variable affected the inductive coupling.

5. Graphs from the data tables were generated, allowing the results to be assessed, and conclusions to be drawn regarding the performance of each design.

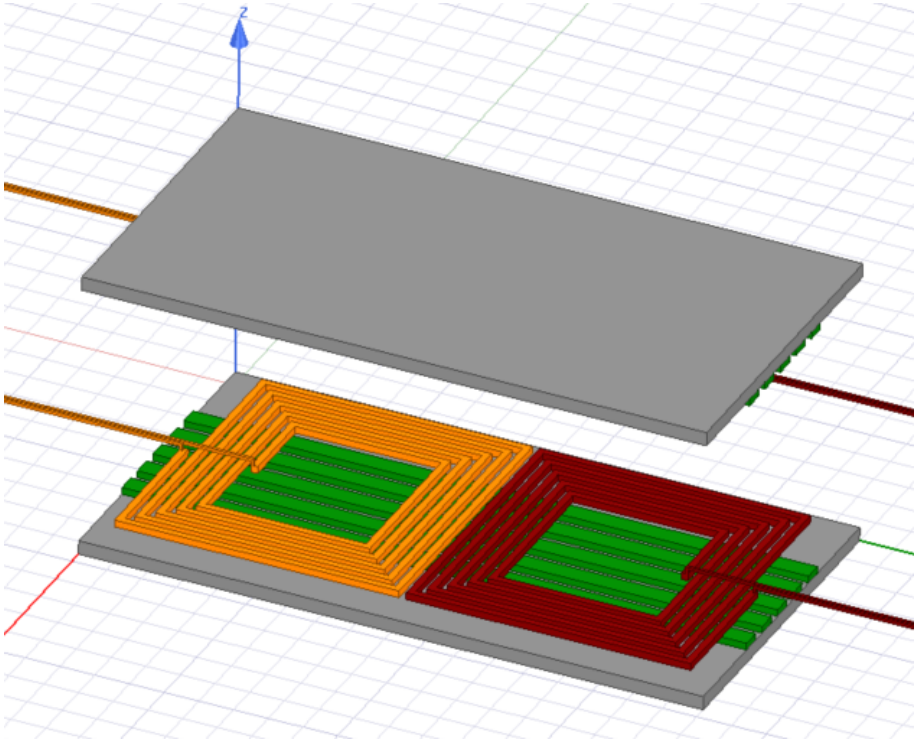

Figure 23: ANSYS model of a DD pad transmitter and receiver

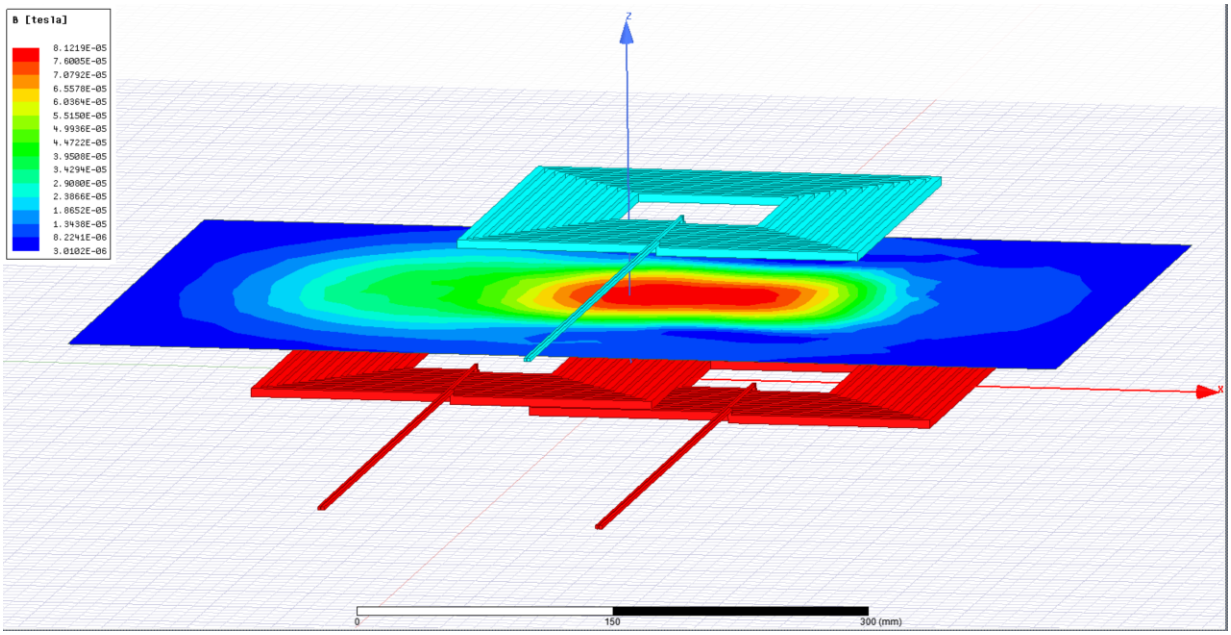

Figure 24: magnetic field intensity heat map

3.3 Small-Scale Resonant System Investigation

Resonant inductive coupling (as opposed to purely inductive coupling) is very difficult to simulate in ANSYS. Hence, to conduct investigations involving resonant inductive coupling, a small-scale resonant system was constructed. The objective was then to critically assess the performance of different small-scale primary and secondary coil designs when utilized within a resonant system.

Technical Approach:

1. Small-scale prototypes of the transmitter and receiver designs which provided the best simulation results in ANSYS were constructed. Figure 25 shows the small-scale prototypes of a DD pad transmitter and a DD pad receiver. For the small-scale prototypes, magnetic shielding was also implemented using a ferrite back-plate, as seen in figure 25.

2. The inductances of the transmitter and receiver coil prototypes were measured using an LCR meter. Additionally, a drive frequency of 400kHz was chosen for the small-scale testing.

3. The primary and secondary compensator circuits (LC resonators) were constructed, by calculating capacitor values using equation 1. This allowed the primary and secondary compensator circuits to resonate at the same frequency.

4. A full-bridge rectifier circuit with fast switching diodes was built and connected to the secondary side compensator circuit.

5. To drive the small-scale system, a 10Vpp square wave was generated. This was achieved using a high slew rate ($75V/\mu s$) operational amplifier to amplify the square wave output from the micro-controller (TIVA). The slew rate of the op-amp needed to be large, since the drive frequency of the system was 400kHz (micro-controller set the drive frequency). Figure 26 depicts the primary side setup used to drive the small scale system. The op-amp, DC power supply (used to power the op-amp), transmitter coil and capacitors for resonance can all be seen in figure 26.

6. Once the resonant system was set up, parameters such as air gap and horizontal misalignment were varied. The system's robustness to these variations was then analysed by measuring power transfer capability and efficiency of power transfer.

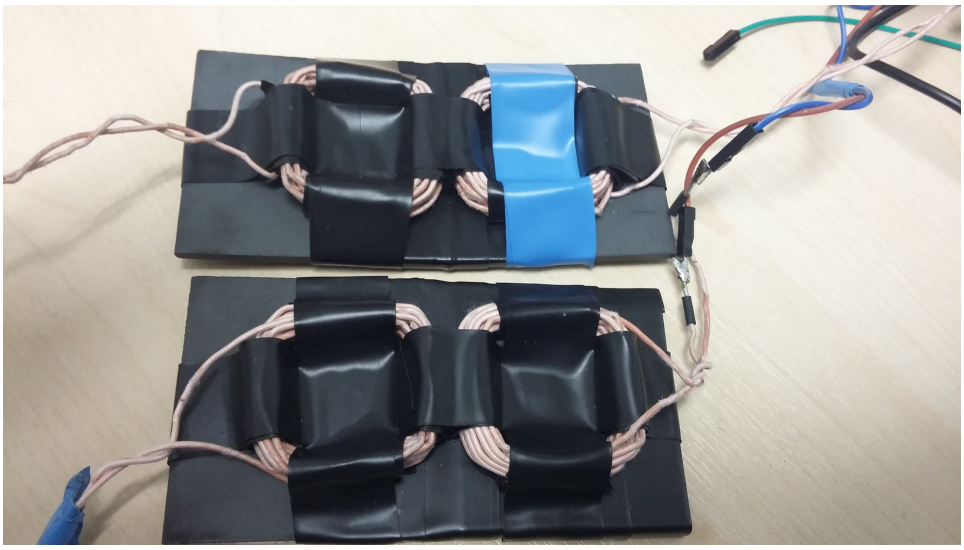

Figure 25: small-scale DD pad transmitter and receiver

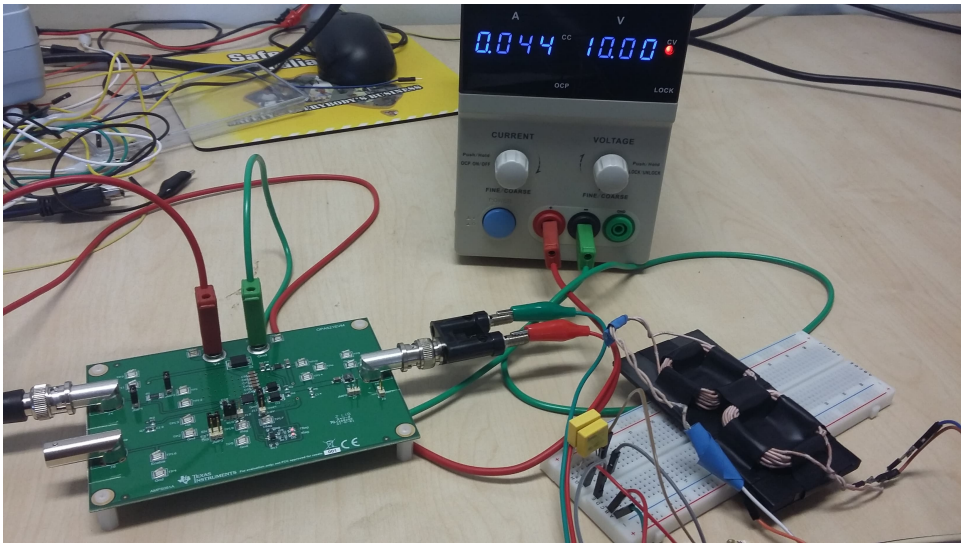

Figure 26: primary side setup used to drive the small-scale system

3.4 Small-Scale Resonant System Tuning

In a dynamic wireless power transfer system, variation in misalignment between the transmitter and receiver causes the mutual inductance between them to change. As a result, the resonant frequency of the system changes as misalignment occurs.

Therefore, the objective for this part of the investigation process was to determine whether resonance tuning could be utilized to improve the small-scale system's robustness to horizontal misalignment.

Technical Approach:

1. The small-scale system used for the resonance tuning investigation is shown in figure 27. The transmitter and receiver were both DD pads. The air gap and movement misalignment were kept constant, since horizontal misalignment was the variable of interest.

2. The resonant frequency at any misalignment is found by adjusting the drive frequency until the power output transferred to the load is at a maximum. Using this method, the resonant frequency was then found for a horizontal misalignment of 0%. This is the original drive frequency.

3. The horizontal misalignment was then varied from 0% to 100%. At each misalignment, the output power was recorded for both the original frequency, and also the fine tuned resonant frequency for the new misalignment.

4. The output power at both the original and fine tuned frequency for each misalignment was then compared graphically. From this data it was possible to determine whether resonance tuning could make significant improvements to a dynamic wireless power transfer system.

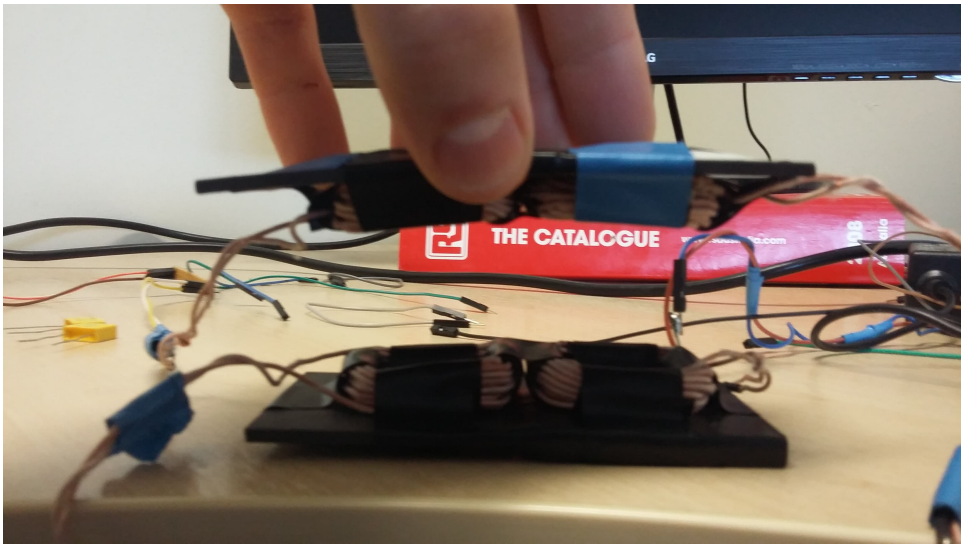

Figure 27: the small-scale DD pads used for the resonance tuning investigation

3.5 Automated Tuning for the Resonant System

The objective of this part of the investigation was to develop a feedback network which allows the system to automatically tune itself to resonance as misalignment occurs. However, to do this, a method for detecting the resonant frequency using **information from only the primary side** was required.

When the system is resonating, the current in the primary side circuit is at a maximum [25]. This is because the impedance of the primary circuit is at a minimum, due to the cancellation of the capacitive and inductive impedances in the compensation filter [25].

Therefore, if the micro-controller which controls the drive frequency of the system can receive data regarding the primary current, resonance tuning can be automated. The current in the compensation filter is very high frequency. Hence, measuring the DC current drawn from the power supply which powers the op-amp was a simpler and more effective approach.

Technical Approach:

1. An ACS712 hall-effect-based current sensor was placed in series with the Vcc output of the DC power supply, and the Vcc input of the op-amp, as demonstrated in figure 28. The current sensor then outputs a scaled analogue voltage based on the current it detects. This analogue voltage was connected to an ADC pin on the TIVA (micro-controller), again demonstrated in figure 28.

2. A state machine was programmed onto the micro-controller which altered the drive frequency so as to keep the ADC voltage reading at a maximum. A visual representation of this state machine is shown in Appendix C. The code used to program this state machine onto the TIVA (micro-controller) is shown in Appendix D.

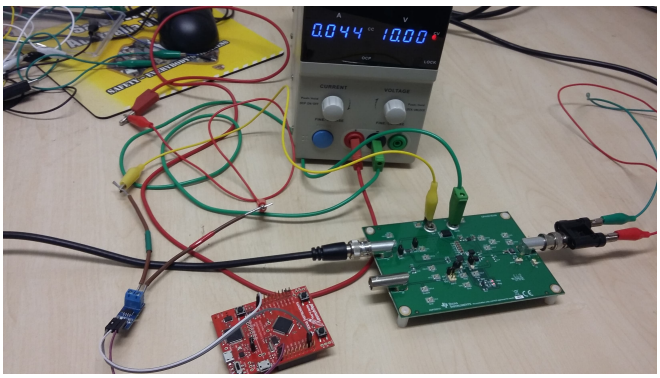

Figure 28: automatic resonance tuning setup: current sensor, TIVA, op-amp, DC power supply

3.6 Segmentation Implementation

The objective of segmentation was to develop a system which could detect the presence of the electric vehicle. This system could then be used to indicate when to turn the primary driver circuit on (as the vehicle arrives) and off (as the vehicle leaves). An additional benefit of the segmentation system is that it could be used to detect the direction of the vehicle's movement.

Figure 29 shows the large-scale charging pad. Currently, it consists of two DD pads, which are both driven by the same source. In figure 29, two magnetometers are also depicted, one on the far left and the other on the far right. The magnetometers used were HMC5883L 3-axis magnetometers.

Figure 30 shows the electric vehicle. At the front of this electric vehicle, a magnet was placed with its north magnetic pole facing down. Also, at the back of the electric vehicle, a magnet was placed with its south magnetic pole facing down.

With the magnetometers placed at the start and end of the charging pad, and the magnets placed at the front and back of the vehicle, the segmentation system was ready to be programmed using the micro-controller (TIVA).

Technical Approach:

1. Firstly, the magnetometers were calibrated by determining the natural magnetic flux density in the vertical direction (z-axis) when no magnets were present.

2. When the vehicle drove over the magnetometers, the magnetic flux density would read above the calibration threshold for the front magnet (north facing down), and below the calibration threshold for the back magnet (south facing down).

3. If magnetometer 1 (figure 29 far left) detected the front magnet first, the micro-controller would turn the system on. The system would then not be turned off until magnetometer 2 (figure 29 far right) detected the back magnet. Hence, the charging pad would be active the whole time the vehicle was over it.

4. Conversely, if magnetometer 2 detected the front magnet first, the micro-controller would turn the system on. The system would then not be turned off until magnetometer 1 detected the back magnet.

5. If magnetometer 1 detected the front magnet first, the vehicle was determined to be travelling in direction A, and if magnetometer 2 detected the front magnet first, the vehicle was determined to be travelling in direction B. Hence, this segmentation system was also capable of distinguishing between two possible directions of movement.

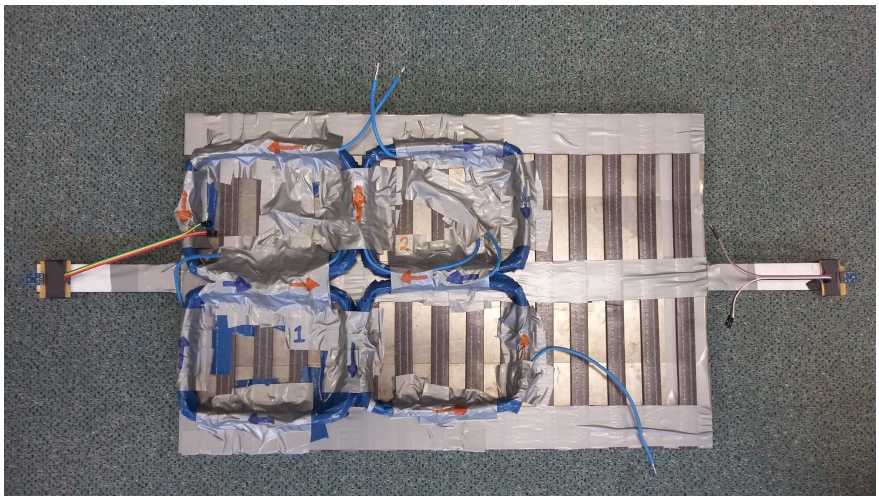

Figure 29: integrated DD charging pads (large scale) with magnetometers for segmentation

Figure 30: The Electric Vehicle

4 Results and Analysis

4.1 Simulation Results

4.1.1 Rectangular Coil Width

This investigation involved using ANSYS to examine how the dimensions of rectangular coils impact the coupling coefficient. The length of both coils, the transmitter and receiver, remained constant at 200mm, the air gap remained constant at 10mm, and the widths were varied from 25mm to 200mm in steps of 25mm. The transmitter and receiver coils remained identical for each width. In ANSYS, resonant coupling is very difficult to simulate, hence, the two coils in these simulations were inductively coupled. The results from the simulations are shown in figure 31.

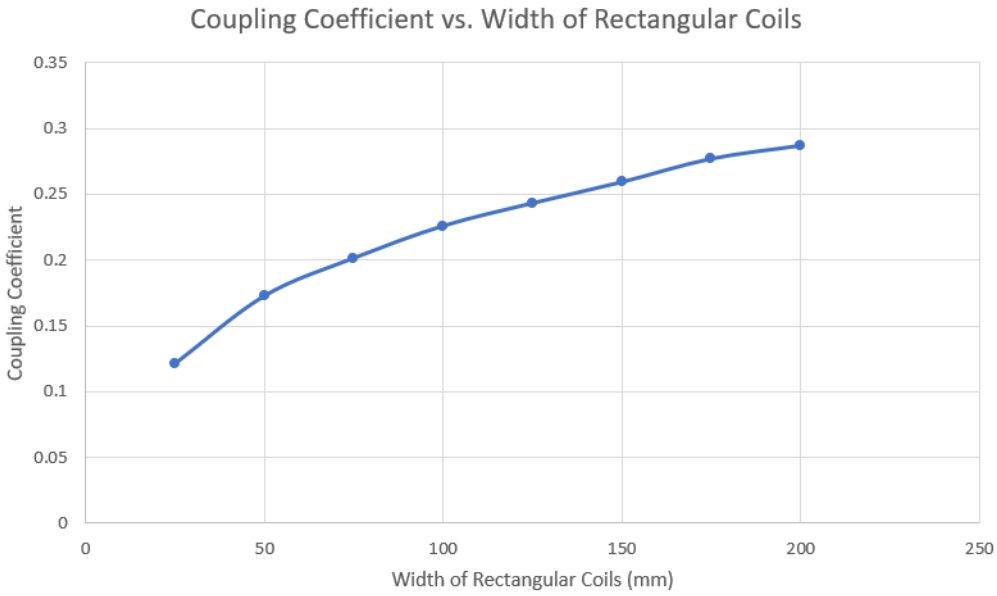

Figure 31: graph displaying coupling coefficient vs width of rectangular coils

Figure 31 demonstrates that as the width of the transmitter and receiver coils increased, the coupling coefficient also increased. The coupling coefficient is at a maximum when the width is equal to the length (width = length = 200mm). Therefore, the results suggest that the best rectangular coil dimensions for inductive coupling are: length = width (square coils - width/length ratio = 1). This result is logical, because rectangular coils with a smaller width/length ratio will have more destructive interference between flux generated from opposite sides of the coil, hence, reducing coupling capabilities [26].

4.1.2 Transmitter-Receiver Separation (Air Gap)

To examine how the coupling coefficient between two coils changes with air gap, two square coils were constructed in ANSYS both with 1 turn and a 120mm side length. The simulation to determine the coupling coefficient was then run for a range of air gaps between 4mm and 200mm. The results are shown in figure 32.

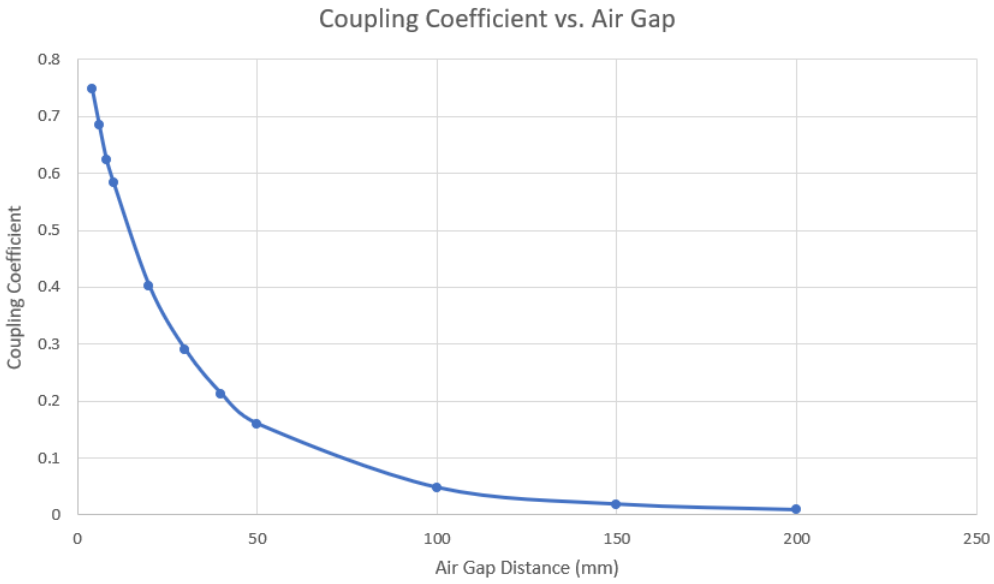

Figure 32: coupling coefficient vs air gap distance for square coils with a 120mm side length

Figure 32 demonstrates an exponential drop-off in coupling coefficient as air gap increases. At an air gap of 4mm, the coupling coefficient is approx 0.75, and at an air gap of 100mm, the coupling coefficient is approx 0.05. These results suggest that the drop-off in coupling coefficient between inductively coupled coils is too significant. This is the primary incentive for wireless power transfer systems to implement resonant inductive coupling rather than pure inductive coupling [5].

4.1.3 Horizontal Misalignment

Figure 33 shows the ANSYS model for a DD charging pad which utilizes ferrite bars and a steel back-plate to direct flux towards the receiver pad. Both of the coils in the DD pad are square, because of the previous results which suggested square coils coupled the most effectively.

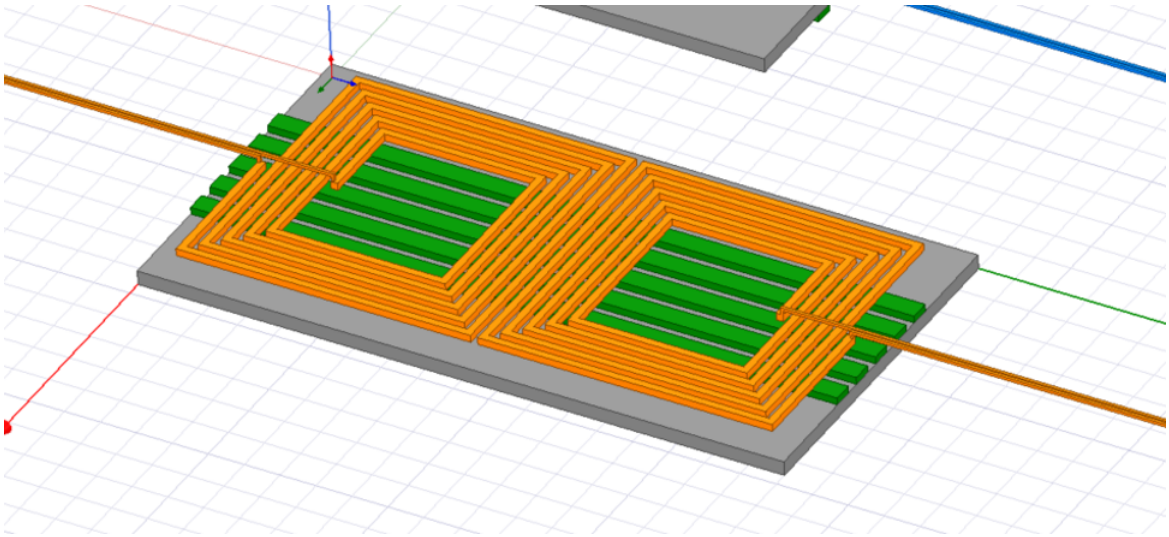

Figure 33: DD charging pad with ferrite bars and steel back-plate

Research suggests that DD charging pads are somewhat effective for reducing susceptibility to horizontal misalignment, however, also suggests that certain dead zones exist (as discussed previously in section 2.5.2). In the following simulations, two DD pads were coupled together over a constant air gap, whilst the horizontal misalignment was varied from 0mm (no horizontal misalignment) to 90mm (100% horizontal misalignment). The results from the simulations are shown in figure 34.

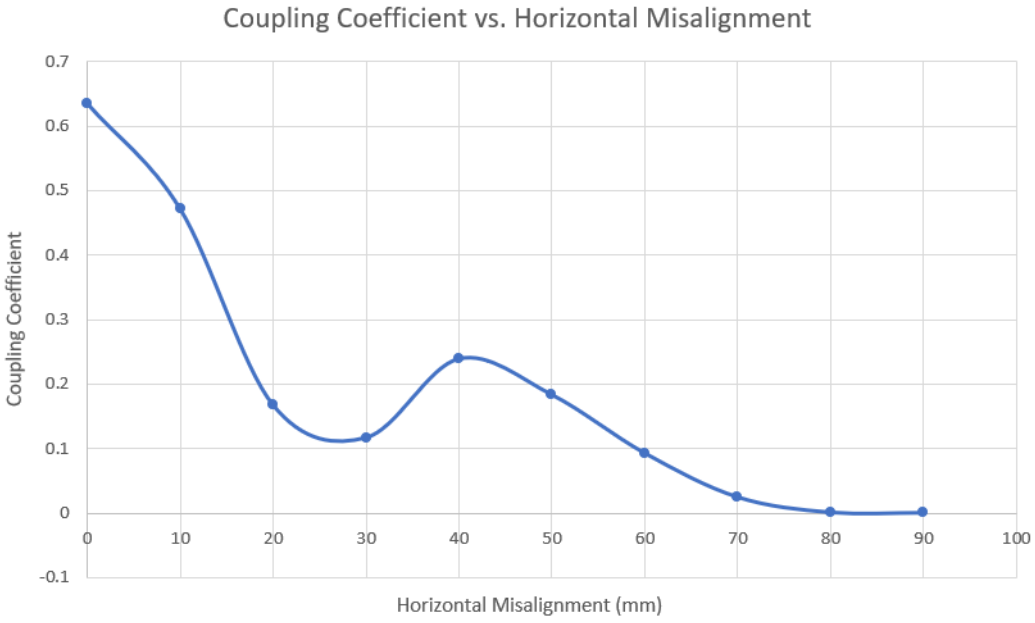

Figure 34: coupling coefficient vs horizontal misalignment (DD to DD coupling)

The results in figure 34 demonstrate the main weakness involved with DD pads and horizontal misalignment. At 25mm of horizontal misalignment (27% misalignment) there is a dead zone. At this point the coupling coefficient has dropped from 0.64 (the coupling coefficient at 0% misalignment) to 0.11. At 40mm of horizontal misalignment (44% misalignment) the coupling coefficient reaches a small peak at 0.24, and then continues to diminish for misalignments greater than 40mm.

To summarise, the results have demonstrated that DD pads have inductive coupling dead zones when horizontal misalignment occurs. However, it is important to note that this ANSYS simulation was simulating inductive coupling, not resonant inductive coupling. When two physical DD pads are resonant inductively coupled, and power is being transferred wirelessly between them, the resonant frequency can be tuned as misalignment occurs, to account for the variation in mutual inductance [27]. This technique can be applied to minimise the dead zones [27]. The next section discusses the results obtained from the investigation performed to eliminate the dead zones associated with DD pads and horizontal misalignment.

4.2 Small-Scale Resonant System Results

4.2.1 Resonance Tuning Investigation

This investigation involved measuring the output power transferred by a small-scale resonant inductive WPT system, at different levels of horizontal misalignment (ranging from 0% to 100%). The transmitter and receiver were both DD pads, as depicted in figure 27 (section 3.4). At each misalignment, the output power was calculated by placing a resistor on the output of the rectifier on the secondary side, measuring the voltage drop across it, and then applying equation 7.

$$P = \frac{V^2}{R} \tag{7}$$

Two tests were conducted. One test implemented resonance tuning, and the other did not. For the test which did not implement resonance tuning, the initial resonant frequency was found by tuning the system to resonance at 0% misalignment. This involved varying the drive frequency until the voltage across the output resistor was maximised. The drive frequency then remained at this original frequency for all levels of misalignment.

For the test which did implement resonance tuning, at every level of misalignment, the new resonant frequency was found (if a new resonant frequency existed), and the output power was recorded at this new frequency. The results for the test which did not utilise resonance tuning are shown in figure 35, and the results for the test which did utilise resonance tuning are shown in figure 36.

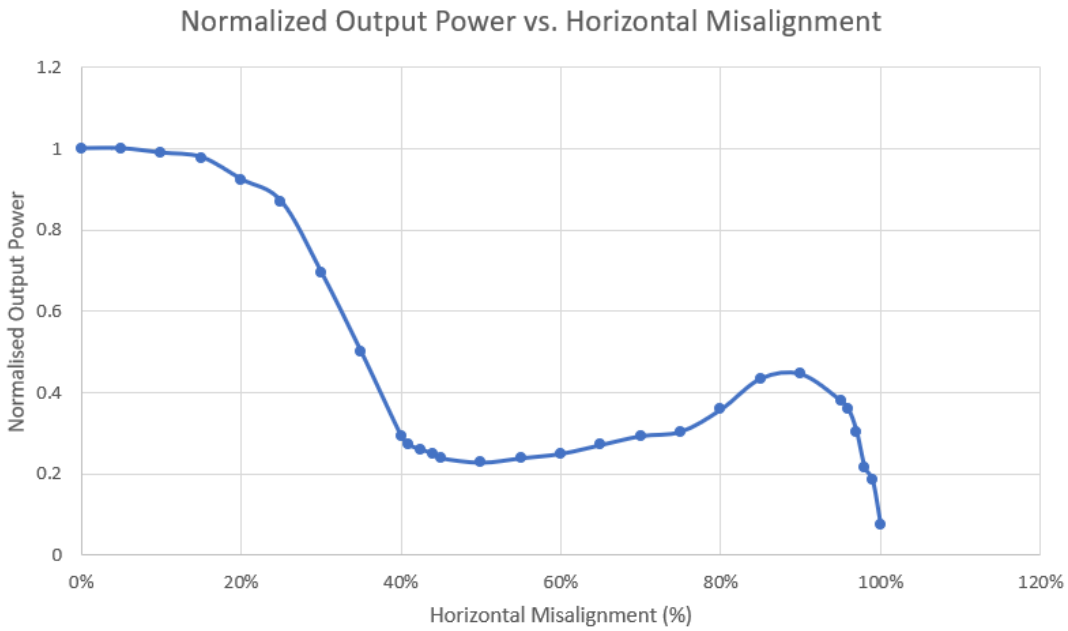

Figure 35: normalised output power vs. horizontal misalignment for a non-resonant-tuned system

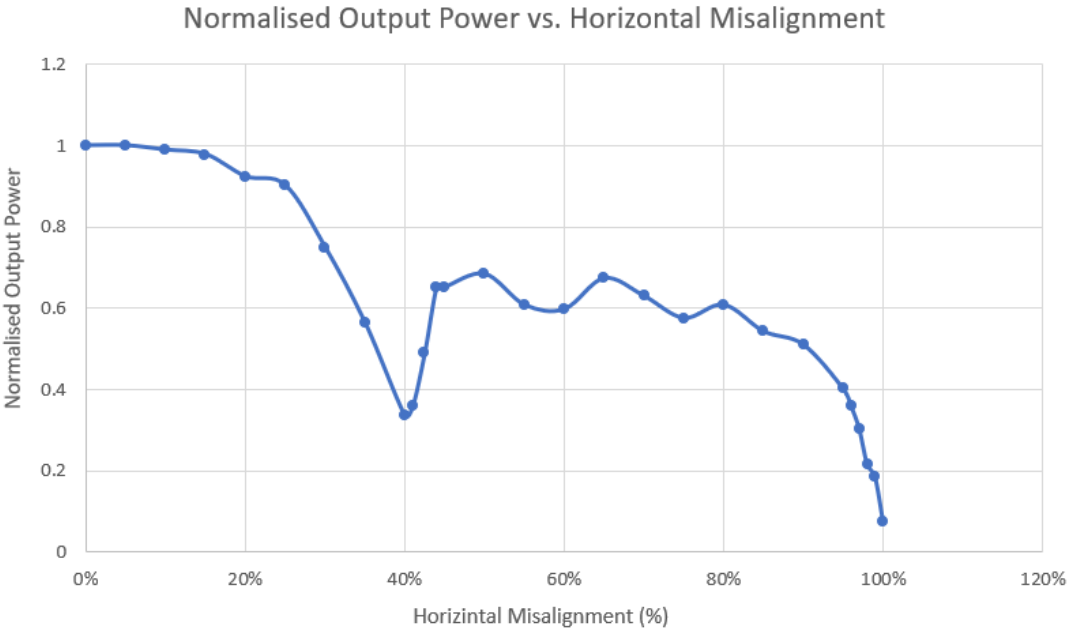

Figure 36: normalised output power vs. horizontal misalignment for a resonant-tuned system

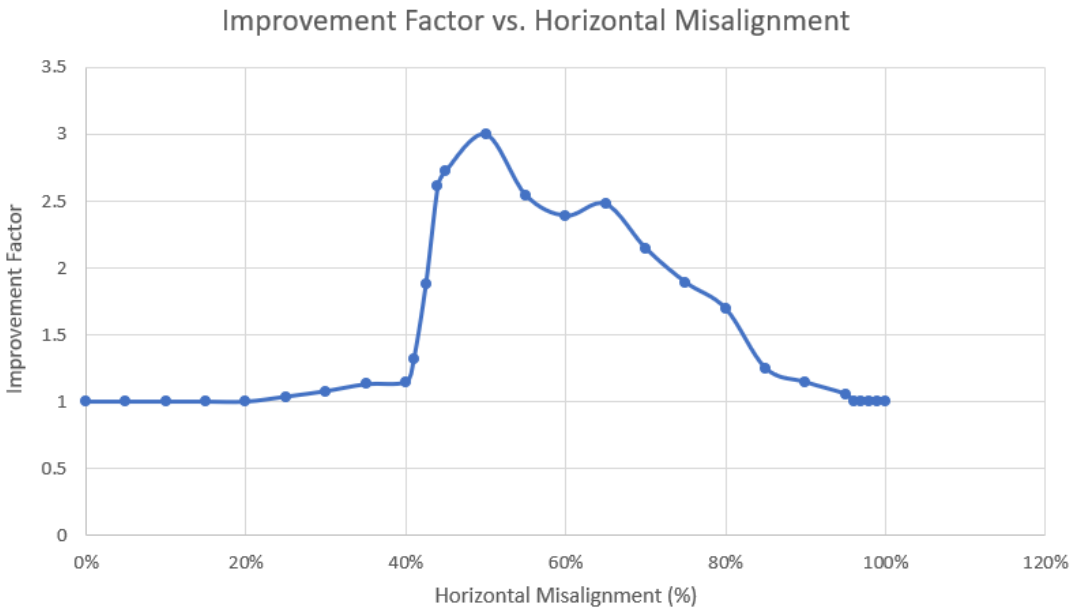

Figure 37: the factor of improvement introduced by resonance tuning vs. horizontal misalignment

Figure 35 shows the normalised output power vs. horizontal misalignment for the non-resonant-tuned system. It can be seen that there is a power transfer dead zone which reaches a minimum at approximately 40% horizontal misalignment. The output power then rises gradually to a small peak at 90% misalignment, then dies off rapidly between 90 and 100% misalignment. These results demonstrate a curve which has a similar shape to the curve obtained from the ANSYS simulation in figure 34.

Figure 36 shows the normalised output power vs. horizontal misalignment for the resonant-tuned system. When compared to the results from figure 35, the output power is much more constant, and the dead zone at 40% misalignment has been significantly reduced. Figure 37 demonstrates the factor of improvement introduced by the resonance tuning at each misalignment. At 50% misalignment, it can be seen that the output power is improved by a factor of 3, which is very significant. Also, from approx. 42% misalignment to 70% misalignment, the improvement factor is consistently above 2. These results clearly demonstrate that by implementing resonance tuning, the system becomes much more robust to horizontal misalignment.

4.2.2 Automatic Resonance Tuning

The final part of this project was the automation of the resonance tuning using the micro-controller. Section 3.5 (in "Project Methodology" section) describes how this was achieved. The state machine depicted in Appendix C and Appendix D, which was programmed onto the micro-controller (TIVA), was effective at locating the resonant frequency automatically, and achieved the same results as in figure 36.

The automatic location of the resonant frequency, however, was not fast enough, when compared to the speed at which an electric vehicle would drive over the charging pads. Hence, improvements need to be made to the automation firmware to improve the speed of the resonant frequency location.

5 Conclusions and Recommendations

Reviewing literature and investigating state-of-the-art systems regarding dynamic wireless power transfer was a considerable portion of this thesis. This is primarily due to the abundance of literature available regarding design characteristics and techniques for systems being optimised for a dynamic wireless charging environment. Numerous conclusions were obtained from the literature alone before any simulations were run or any real-life experiments were conducted. These included:

1. A resonant inductive wireless power transfer system was the optimal topology for the wireless charging of an electric vehicle. This was primarily due to its capabilities of achieving strong coupling over large air gaps (several times the coil diameter), which is important for electric vehicle charging.

2. A DD to DDQ transmitter-receiver topology was the most effective for improving the system's robustness to horizontal misalignment (delivering a more constant output power w.r.t horizontal misalignment). The management of the power transferred to a DDQ receiver, however, requires more complicated circuitry, which must be taken into consideration.

3. A crossed DD to DDQ transmitter-receiver topology was the most effective for improving the system's robustness to both horizontal and vertical misalignment (delivering a more constant output power w.r.t horizontal and vertical misalignment). Winding the DD coils for a crossed DD pad transmitter, however, can be difficult to achieve without flux cancellations.

4. Utilizing Litz wire minimises the skin effect, and allows the system to be driven at a higher frequency. A higher drive frequency improves the quality factor of the coils, and by extension, the efficiency of the power transfer. Litz wire, however, is not cheap, which is a major design consideration.

5. Utilizing metallic and magnetic shielding to reduce leakage flux are techniques which will improve the efficiency of the system considerably. However, for these techniques, budget is a large consideration, as large quantities of ferrite and metal (aluminium or steel) can be expensive.

After the research phase, the next phase was using ANSYS Electronics desktop to run simulations involving inductive coupling between different transmitter and receiver coils. Firstly, the coupling between a rectangular transmitter and receiver was simulated. From this simulation, it was deduced that square coils have the strongest coupling, hence, rectangular coils should always be constructed with a width/length ratio of 1. To conclude, when constructing DD pads, it is important to ensure that both "D coils" have a square geometry.

The second simulation investigated inductive coupling w.r.t a changing air gap. It was concluded that the drop-off in coupling strength as the air gap increased was very significant . This confirmed the research which suggested that resonant inductive coupling was utilized to counter the air gap limitations involved with pure inductive coupling. Hence, it was concluded that the real-life prototypes would achieve stronger coupling by employing the use of a resonant circuit topology.

The final simulation investigated inductive coupling between a DD pad transmitter and a DD pad receiver, whilst horizontal misalignment was varied. It was concluded from this investigation that a coupling dead zone existed at 27% horizontal misalignment. This result supported the research which suggested that DD pads encounter a coupling dead zone as horizontal misalignment occurs.

The DD pad simulation result inspired the next investigation, which involved applying resonance tuning to a real-life DD to DD prototype, and attempting to minimise the dead zone. It was concluded from this investigation that resonance tuning is a very effective technique for removing dead zones, and providing a more constant output power as horizontal misalignment occurs.

Through an assessment of the various conclusions drawn from investigations conducted throughout this project, recommendations have been formulated to guide future research. These include:

1. When resonance tuning was applied to a DD to DD topology, the system's robustness to horizontal misalignment was improved. Additionally, research suggested that a DD to DDQ topology is more robust to horizontal misalignment than a DD to DD topology without resonance tuning. Therefore, for maximum robustness to horizontal misalignment, a DD to DDQ topology which also implements resonance tuning would be very effective.

2. Research suggested that a crossed DD pad transmitter improves the system's robustness to movement misalignment. Hence, a system which utilizes a crossed DD pad transmitter, a DDQ pad receiver, and resonance tuning, would be very robust to **both horizontal and movement misalignment**. Investigating this topology in ANSYS and testing a prototype system would likely lead to a design which is very effective for dynamic wireless power transfer. The main objective with the ANSYS simulations would be to ensure there are no flux cancellations involved with the winding of the crossed DD pad transmitter.

3. In this project, the segmentation system used magnetometers to detect the presence of the electric vehicle. This was discussed in section 3.6. The magnetic flux generated by the charging coils interfered with the magnetometers, and as a result, the magnetometers had to be placed a significant distance from the

coils, as depicted in figure 29. Therefore, a recommendation for future development would be to use a different detection system, perhaps an optical sensor.

6 References

[1] D. M. Clarke, "Cable hanger for electrically powered mine vehicles," Jul. 11 1989, uS Patent 4,846,320.

[2] S. Sinha, B. Regensburger, K. Doubleday, A. Kumar, S. Pervaiz, and K. K. Afridi, "High-power-transfer-density capacitive wireless power transfer system for electric vehicle charging," in *2017 IEEE Energy Conversion Congress and Exposition (ECCE)*. IEEE, 2017, pp. 967–974.

[3] C. Panchal, S. Stegen, and J. Lu, "Review of static and dynamic wireless electric vehicle charging system," *Engineering science and technology, an international journal*, 2018.

[4] J. Dai and D. C. Ludois, "A survey of wireless power transfer and a critical comparison of inductive and capacitive coupling for small gap applications," *IEEE Transactions on Power Electronics*, vol. 30, no. 11, pp. 6017–6029, 2015.

[5] A. Kurs, A. Karalis, R. Moffatt, J. D. Joannopoulos, P. Fisher, and M. Soljačić, "Wireless power transfer via strongly coupled magnetic resonances," *science*, vol. 317, no. 5834, pp. 83–86, 2007.

[6] S. Li and C. C. Mi, "Wireless power transfer for electric vehicle applications," *IEEE journal of emerging and selected topics in power electronics*, vol. 3, no. 1, pp. 4–17, 2015.

[7] G. Ceglia, V. Guzmán, C. Sanchez, F. Ibanez, J. Walter, and M. I. Giménez, "A new simplified multilevel inverter topology for dc–ac conversion," *IEEE transactions on power electronics*, vol. 21, no. 5, pp. 1311–1319, 2006.

[8] H. A. Wheeler, "Formulas for the skin effect," *Proceedings of the IRE*, vol. 30, no. 9, pp. 412–424, 1942.

[9] J. Ferreira, "Analytical computation of ac resistance of round and rectangular litz wire windings," in *IEE Proceedings B (Electric Power Applications)*, vol. 139, no. 1. IET, 1992, pp. 21–25.

[10] M. Budhia, J. T. Boys, G. A. Covic, and C.-Y. Huang, "Development of a single-sided flux magnetic coupler for electric vehicle ipt charging systems," *IEEE Transactions on Industrial Electronics*, vol. 60, no. 1, pp. 318–328, 2013.

[11] L. Zhao, S. Ruddell, D. J. Thrimawithana, U. K. Madawala, and P. A. Hu, "A hybrid wireless charging system with ddq pads for dynamic charging of evs," in *2017 IEEE PELS workshop on emerging technologies: wireless power transfer (WoW)*. IEEE, 2017, pp. 1–6.

[12] L. Xiang, Y. Sun, C. Tang, X. Dai, and C. Jiang, "Design of crossed dd coil for dynamic wireless charging of electric vehicles," in *2017 IEEE PELS Workshop on Emerging Technologies: Wireless Power Transfer (WoW)*. IEEE, 2017, pp. 1–5.

[13] J. Kim, J. Kim, S. Kong, H. Kim, I.-S. Suh, N. P. Suh, D.-H. Cho, J. Kim, and S. Ahn, "Coil design and shielding methods for a magnetic resonant wireless power transfer system," *Proceedings of the IEEE*, vol. 101, no. 6, pp. 1332–1342, 2013.

[14] J. Paraszczak, E. Svedlund, K. Fytas, and M. Laflamme, "Electrification of loaders and trucks–a step towards more sustainable underground mining," in *Proceedings of the International Conference on Renewable Energies and Power Quality (ICREPQ'14), Cordoba, Spain*, 2014, pp. 7–10.

[15] F. N. Ibrahim, N. Jamail, and N. Othman, "Development of wireless electricity transmission through resonant coupling," 2016.

[16] F. Lu, H. Zhang, and C. Mi, "A two-plate capacitive wireless power transfer system for electric vehicle charging applications," *IEEE Transactions on Power Electronics*, vol. 33, no. 2, pp. 964–969, 2018.

[17] H. Wu, A. Gilchrist, and K. Sealy, "Wireless power transfer magnetic couplers," Jan. 19 2016, uS Patent 9,240,270.

[18] S. Sasaki, K. Tanaka, and K.-i. Maki, "Microwave power transmission technologies for solar power satellites," *Proceedings of the IEEE*, vol. 101, no. 6, pp. 1438–1447, 2013.

[19] electronics tutorials, "Transformer basics," in *Website*. www.electronics-tutorials.ws, 2019, accessed: 25-02-2019. [Online]. Available: https://www.electronics-tutorials.ws/transformer/transformer-basics.html

[20] C. M. Zierhofer and E. S. Hochmair, "Geometric approach for coupling enhancement of magnetically coupled coils," *IEEE transactions on Biomedical Engineering*, vol. 43, no. 7, pp. 708–714, 1996.

[21] electronics notes, "Inductor quality factor," in *Website*. Electronics-notes.com, 2019, accessed: 25-02-2019. [Online]. Available: https://www.electronics-notes.com/articles/basic$_c$*oncepts*/$q - quality - factor$/$inductor - q - factor.php$

[22] M. Bartoli, N. Noferi, A. Reatti, and M. K. Kazimierczuk, "Modeling litz-wire winding losses in high-frequency power inductors," in *PESC Record. 27th Annual IEEE Power Electronics Specialists Conference*, vol. 2. IEEE, 1996, pp. 1690–1696.

[23] G. Ke, Q. Chen, L. Xu, S.-C. Wong, and K. T. Chi, "A model for coupling under coil misalignment for dd pads and circular pads of wpt system," in *2016 IEEE Energy Conversion Congress and Exposition (ECCE)*. IEEE, 2016, pp. 1–6.

[24] J. Huh and C.-T. Rim, "Kaist wireless electric vehicles-olev," SAE Technical Paper, Tech. Rep., 2011.

[25] P. Gibbs, "Systems and methods for automated resonant circuit tuning," Jan. 5 2006, uS Patent App. 11/168,296.

[26] M. Budhia, J. T. Boys, G. A. Covic, and C.-Y. Huang, "Development of a single-sided flux magnetic coupler for electric vehicle ipt charging systems," *IEEE Transactions on Industrial Electronics*, vol. 60, no. 1, pp. 318–328, 2011.

[27] Z. Qian, R. Wang, Z. Wang, J. Du, J. Wu, and X. He, "Closed-loop control design for wpt system using power and data frequency division multiplexing technique," in *2016 IEEE Energy Conversion Congress and Exposition (ECCE)*. IEEE, 2016, pp. 1–5.

7 Appendices

Appendix A: Professional Development

Before starting my placement at Mining3, I had never worked as an engineer or experienced a professional engineering environment. Hence, this semester has been a huge learning experience for me. Overall, I am very grateful that I was granted the opportunity to complete an industry placement, as it has allowed me not only to develop useful technical skills, but also build my confidence in a professional environment and improve my professional demeanour.

At Mining3, I completed my placement alongside 3 other students from UQ, and one student from QUT. We all started off the project by researching and discussing ideas as a group. Since we were all working on the same project, and felt very comfortable around one another, it was very easy to forget to branch out to the rest of the engineers at Mining3, and only discuss issues and complications with one another. However, as the semester went by, I became more and more familiar with the rest of the engineers at Mining3, by seeing them at lunch, stand-up meetings, learning lunches, research seminars, or even just around the workplace in general. Being familiar with the other engineers made it easier to ask them for help and guidance, which was always useful, as there are many talented and knowledgeable engineers at Mining3.

During this placement, I learnt a great deal about time management. It was important to always be planning, and allocating time accordingly to different tasks. For example, some weeks I would spend more time researching, other weeks, I would be building, testing, ordering components, etc. Then, when it came to the weeks when university assessment was due (reflections, project proposal, interim report, final report), I would have to put other tasks on hold for a while to focus on writing detailed reports. Hence, it was important to be constantly aware of what tasks needed to be prioritised, in order to reach the goals I had planned out in my project timeline. In hindsight, 24 weeks seemed like a long time, however, when you consider the aspects of a project: the learning curve, the research, coming up with ideas, throwing away bad ideas, simulating, ordering components and waiting for them, constructing, testing, remodelling designs, etc, you realise that time is a precious resource and must be managed wisely.

Table 3 shows a summary of all the learning events which I reflected upon during this placement, what month they took place in, and the EA stage 1 competencies developed during each learning event. Analysing table 3 gives an idea of how my learning progressed and changed throughout this placement.

Month	Learning Event	EA Stage 1 Competencies Developed
February	Preparing Myself for an Effective Work Day	EA 3.5
February	Attending a Learning Lunch	EA 1.6
February	Receiving a Lab Safety Induction	EA 2.4 and EA 3.1
February	Project Orientated Teamwork	EA 3.6
March	Writing a Project Proposal	EA 3.2 and EA 3.4
March	Safety Share at the Monday Morning Stand-up Meeting	EA 1.6 and EA 3.1
March	Technical Committee Visited Mining3	EA 2.4 and EA 3.6
March	Supervisor Meeting at Mining3	EA 1.6 and EA 3.5
April	Workplace Risk Assessment	EA 3.1 and EA 3.5
April	Supervisor Working Overseas	EA 3.3 and EA 3.5
April	Purchase Order	EA 2.4 and EA 3.4
April	Discussion of Career Paths with Mining 3 Employees	EA 3.3
May	Problem with Relay Circuit	EA 1.5
May	Remaining Focused with Holiday Distractions	EA 3.3 and EA 3.5
May	Living out of Home	EA 3.5
May	Low Power Testing	EA 1.4 and EA 2.3
June	Research Methodology Seminars	EA 1.4, EA 1.5, and EA 1.6
June	Safescape Presentation at Mt Cotton Training Centre	EA 3.2 and EA 3.3
June	Audio Amplifier Limitations	EA 1.1 and EA 2.1
June	Discussing Weekly Work at Stand-Up Meetings	EA 3.3 and EA 3.5

Table 3: Summary of Learning Events and EA Competencies Developed

In February, table 3 shows that I started off by reflecting on events that were new to me, in terms of starting a new job as a student engineer. The lab safety induction was one of the most thorough inductions I had ever received. It was not like at university, where you can simply do a quiz online and be fully inducted. This made me realise how important safety was within the workplace. In February, I also learnt how to effectively prepare myself for a successful workday, by ensuring I was organised not only at work, but outside of work as well. I attended my first ever learning lunch in February, which taught me that Mining3 was very focused on keeping their workplace community informed and connected.

In March there were a lot of visits to the company. The technical committee came to review projects and discuss future outcomes, and also UQ staff came to Mining3 to discuss how the student projects were coming along. These two visits made me realise that when you are working on a project, conducting research, etc, there are always people who are interested in how you are progressing. Therefore, it is impor-

tant to always be ready to briefly explain to other people how you are progressing and where you are headed with the project. On another note, I was continuously reminded about the importance of safety, after hearing lots of people delivering safety shares at the Monday morning stand-up meetings each week.

In April I placed my first purchase order, as I was keen to start testing some of my initial designs. This event taught me that there is a confirmation process which must be followed in order to buy components. This is because for each project, budget is very important, and items cannot be ordered without a detailed reason. Again, in April I was reminded of the importance of safety, when our supervisor formally took us into a conference room to conduct a proper risk assessment for the project.

In May I started to reflect on events involving the technical work I was doing for my project. This is because in May, I was stressed about the completion of my project. I reflected on a failed circuit which I attempted to use to drive the wireless power transfer system, and also some complications I had to overcome regarding results for my interim report. As a result, May is the month where I did the largest amount of technical learning and developed my skill-set as an electrical engineer. This is because the best learning occurs when you have to overcome and solve problems.

Finally, June was the month where I learned a great deal about presentations, and communicating ideas to other people, colleagues, supervisors, companies, etc. The research methodology seminars hosted by Paul Wilson were very insightful, as Paul Wilson is very effective at communicating his content and engaging an audience. I applied the communications skills I learnt from watching him to the presentation I had to give for university. Another event which taught me a great deal about presenting was the Safescape presentation at Mt Cotton training centre which our supervisor took us to. The Safescape engineers were very effective at selling their product, and communicating with the audience their vision for the implementation of the product in the mining industry. From this even I learnt a great deal about radiating confidence during presentations by being well informed about the subject matter.

Table 3 depicts all the EA stage 1 competencies that I developed throughout this placement. From the Knowledge and Skill Base section I developed EA 1.1, 1.4, 1.5, and 1.6. Hence, I developed my knowledge and skill base quite thoroughly, although there are still two areas to be addressed in the future (EA 1.2 and 1.3). From the Engineering Application Ability section I developed EA 2.1, 2.3, and 2.4 (only missed EA 2.2). Hence, my development was quite thorough in this area. Lastly, from the Professional and Personal Attributes section, had some level of development in all 6 competencies. Therefore, in conclusion, this placement primarily assisted me in developing my professional and personal attributes, which is expected, since I had never worked in a professional engineering environment before.

Appendix B: Project Management

Appendix B.1: Project Timeline

The overall project can be deconstructed into numerous sub-tasks. Tables 4 and 5 describe what each sub-task involves, as well as the estimated time required for completion. Figure 38 then provides a visual representation of the the timeline information presented in tables 4 and 5.

In figure 38, the start of the orange section represents the week in which a particular task is to be started. The end of the orange section is the expected finish week.

Task	**Estimated Time Frame**	**Description**
Literature Review	Week 1 - Week 4 (4 weeks)	Researching the current state of the art for dynamic wireless charging systems, and collating information relevant to the project.
ANSYS Simulations	Week 2 - Week 7 (6 weeks)	The modelling and simulation of different primary and secondary coil geometries and arrangements using ANSYS Electronics Desktop.
Hauler Detection	Week 4 - Week 5 (2 weeks)	The development of a method to detect when the hauler is about to drive over a particular primary coil.
Coil Switching	Week 4 - Week 5 (2 weeks)	Designing a circuit to turn the primary coils on and off based on the presence/absence of the hauler. Used in conjunction with the hauler detection.
Project Proposal	Week 6 - Week 8 (3 weeks)	Writing a report which outlines the context of the project, presents the required outcomes, and defines a plan to achieve the project goals.
Small Scale Primary Side Driver Circuit Construction	Week 9 - Week 11 (3 weeks)	Developing circuitry which can drive the small-scale primary coil with a high frequency square wave.
Small Scale Primary and Secondary Coil Construction	Week 10 - Week 12 (3 weeks)	Building the primary and secondary small-scale coils based on the geometries and arrangements investigated in ANSYS.

Table 4: Project Timeline - First Half of Placement

Task	**Estimated Time Frame**	**Description**
Initial Small-Scale Testing	Week 13 (1 week)	Measuring the efficiency of the resonant inductive power transfer from the primary side to the secondary side. Identifying where improvements can be made.
Remodelling and Optimisation	Week 14 - Week 17 (4 weeks)	After the small-scale testing, the weak spots in the design can be pinpointed. Improvements can then be made by remodelling and re-investigating these weaker areas of the design.
Interim Report	Week 16 - Week 17 (2 weeks)	Report the results from the initial small-scale testing, and perform a progress check by comparing current progress with the timeline from the project proposal.
Large Scale Construction	Week 18 - Week 20 (3 weeks)	Scale-up the successful small-scale system prototypes to 1kW wireless charging systems.
Frequency Feedback Network	Week 20 - Week 22 (3 weeks)	Designing a frequency adjusting feedback network to maintain resonance as the vehicle moves over the primary coils.
Moving Secondary Plate	Week 20 - Week 22 (3 weeks)	If project progress is on schedule, the final task is to develop a method to lower the secondary coil, when the hauler drives over a primary coil.
Final Report	Week 20 - Week 24 (5 weeks)	A large portion of time towards the end of the placement will be dedicated towards writing the final thesis.
Oral Presentation	Week 22 - Week 24 (3 weeks)	At the end of the project, an oral presentation will be given which conveys the important aspects of the thesis/project.

Table 5: Project Timeline - Second Half of Placement

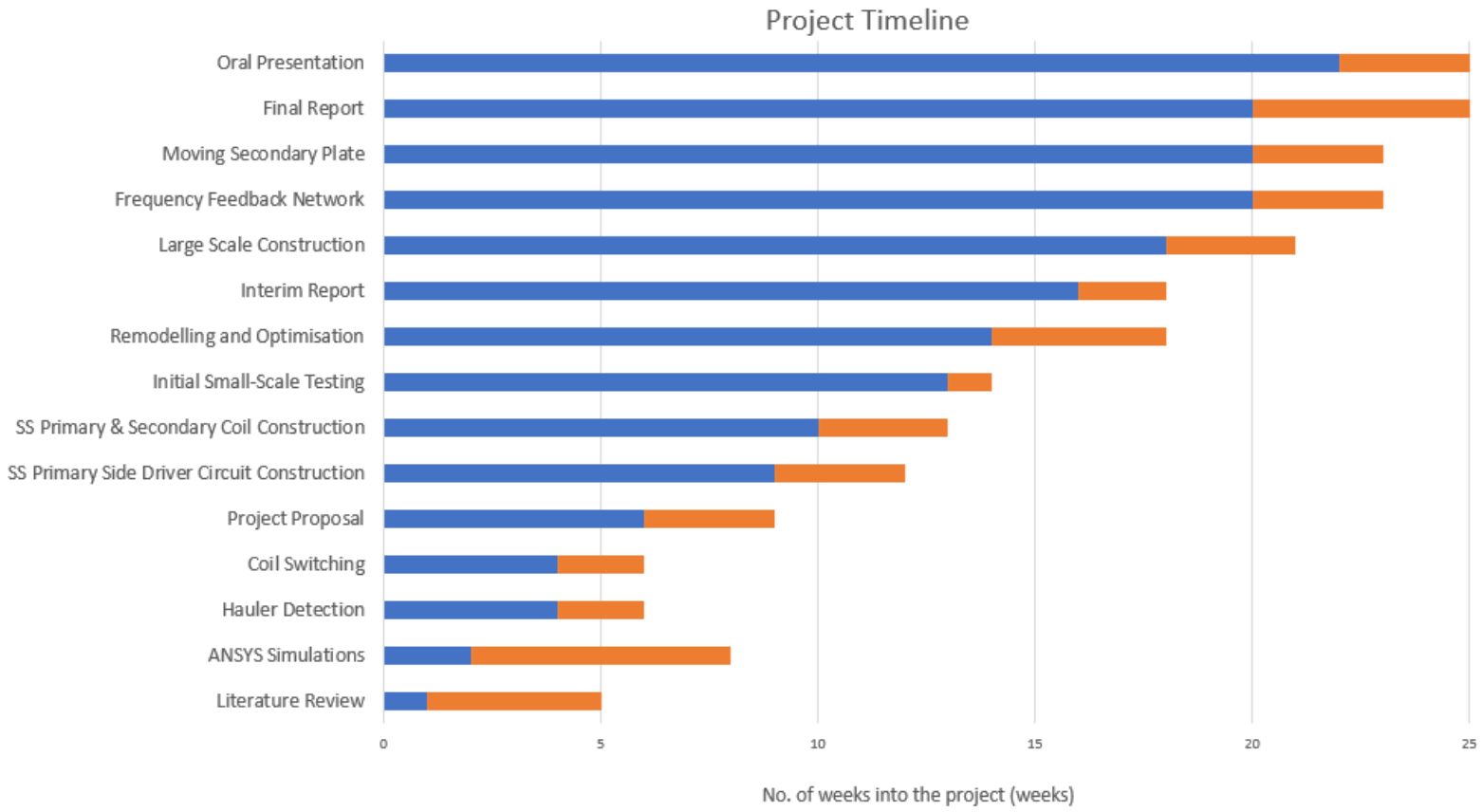

Figure 38: Graphical Representation of the Project Timeline (Gantt Chart)

Appendix B.2: Risk Management

Table 6 is the Mining3 risk assessment matrix. At Mining 3, risks are grouped into four different categories: harm to people, environmental impact, asset damage, and impact on reputation. The risk level can be either low, medium, high, or extreme, depending on both the potential consequence, and the likelihood of occurrence.

The Mining3 risk assessment matrix was used to perform the risk analysis for this project. The first step of the risk analysis was to meet with the rest of the student team and our supervisor, Erik Isokangas, to identify all the potential risks involved with the autonomous hauler project. The second step was to determine the likelihood of each identified risk, and use this to evaluate the corresponding risk rating using the risk assessment matrix. **Table 7 displays the results from the risk analysis**.

		Hazard Effect/ Consequence				
Loss Type		**1 Insignificant**	**2 Minor**	**3 Moderate**	**4 Major**	**5 Catastrophic**
(P) Harm to People		Slight injury or health effects – first aid/ minor medical treatment level	Minor injury or health effects – restricted work or minor lost workday case	Major injury or health effects – major lost workday case/ permanent disability	Permanent total disabilities, single fatality	Multiple fatalities
(E) Environmental Impact		Environmental nuisance	Material environmental harm	Serious environmental harm	Major environmental harm	Extreme environmental harm
(A) Asset Damage & Other Consequential Losses		Slight damage <$5000. No disruption to operation	Minor damage $5000 to $50,000. Brief disruption to operation	Local damage $50,000 to $500,000. Partial shutdown	Major damage $500,000 to $1M. Partial loss of operation	Extreme damage > $1M. Substantial or total loss of operation
(R) Impact on Reputation		Slight impact – public awareness may exist but no public concern	Limited impact – some local public concern	Considerable impact – regional public concern	National impact – national public concern	International impact – international public attention
Likelihood	**Likelihood Examples** (use only as a guide for evaluation of uncontrolled hazards)	**Risk Rating**				
A (Almost certain)	Likely that the unwanted event could occur several times per year at this location	**15 (M)**	**10 (H)**	**6 (H)**	**2 (Ex)**	**1 (Ex)**
B (Likely)	Likely that the unwanted event could occur several times per year in Mining3; or could happen annually	**19 (M)**	**14 (M)**	**9 (H)**	**4 (Ex)**	**3 (Ex)**
C (Possible)	The unwanted event could well have occurred in the mining industry at some time in the past 10 years	**22 (L)**	**18 (M)**	**13 (H)**	**8 (H)**	**5 (Ex)**
D (Unlikely)	The unwanted event has happened in the mining industry at some time; or could happen in 100 years	**24 (L)**	**21 (L)**	**17 (M)**	**12 (H)**	**7 (H)**
E (Rare)	The unwanted event has never been known to occur in the mining industry; or is highly unlikely that it could ever occur	**25 (L)**	**23 (L)**	**20 (M)**	**16 (M)**	**11 (H)**

Risk Matrix Rating	**Risk Level**	**Mining3 Risk Management control guide**
1 to 5	(Ex) – Extreme - Immediate correction required - Eliminate, avoid or implement specific plans/ Standards to manage & monitor	Recommend implementation - minimum of 2 hard control Barriers and 2 soft controls
6 to 13	(H) – High - Should receive attention as soon as possible - Proactively manage	Recommend implementation - minimum of 2 hard control Barriers and 2 soft controls
14 to 20	(M) – Medium - Should be dealt with as soon as possible but situation is not an emergency - pro actively manage	Recommend implementation - minimum of 1 hard control Barriers and 2 soft controls
21 to 25	(L) – Low - Risk is normally acceptable - Monitor & manage as appropriate	Monitor and Manage

Table 6: Mining 3 Risk Assessment Matrix

Task	Potential Hazards	Existing Controls	Risk Rating	Additional Controls	New Risk Rating
Soldering	Solder in eyes.	Safety glasses to protect eyes. Other PPE.	20 (M)	Soldering training. Eye wash station.	23 (L)
	Inhaling solder fumes.	Ventilation to mitigate fumes.	25 (L)		25 (L)
Electronic Testing	Short circuits causing fire/smoke, leads to a potential for burns.	Fire extinguisher. Fuses and circuit breakers.	22 (L)		22 (L)
	Electrical shock.	Use an earth leakage circuit breaker and wear PPE.	18 (M)	Prior to construction, get design verified by an electrical engineer.	22 (L)
Moving/ Lifting	Muscle injury.	Refrain from lifting items heavier than 20kg.	18 (M)	Students receive lifting training.	22 (L)
	Tripping.	Keep work area clean and tidy.	22 (L)		22 (L)
Vehicle Operation	Person to vehicle collisions.	Minimise speeds. Integrate collision avoidance algorithms. Implement remote control operation in case of emergency.	17 (M)	Operate vehicle in a fenced off area.	21 (L)
	Electromagnetic fields interfering with electronic devices. E.g. pacemakers.	Measure field strength to quantify hazard. Implement E-stop switch for coil driver power supply.	18 (M)	Integrate a system into the primary coils so they only turn on when the electric vehicle drives over.	23 (L)
	Lithium batteries or super-capacitors exploding from excessive heat.	Use heat sinks. Store electric vehicle away from heat sources.	17 (M)	Use fireproof bag for charging and storing the batteries. Supercapacitor circuit reviewed by electrical engineer.	21 (L)
Intellectual Property	Theft of IP	Private Dropbox, repositories. IP contracts with UQ.	24 (L)		24 (L)

Table 7: Risk Analysis

Appendix B.3: Resource Requirements

Table 8 lists all the available resources, and explains the necessity of each resource with the respect to the completion of the project.

Resource	**Description**
ANSYS Electronics Desktop	Licence provided by UQ. Used for simulating primary and secondary coil designs.
Laptop	Self provided. Used for research, simulations, report writing, and dropbox file sharing.
Oscilloscope	Mining 3 provided. Used for measuring voltage wave-forms when testing circuitry within the induction system.
Analog Discovery 2	Self provided. Used for debugging small scale signals when programming the hauler detection embedded system.
Electronics Lab	Mining 3 provided. Contains a soldering station and other useful electronic equipment. Used for all circuit construction and soldering.
Mobility Scooter	Mining 3 provided. The mobility scooter is the prototype vehicle being automated and used to demonstrate the dynamic wireless charging.
Reports from previous students	Mining 3/UQ provided. The final reports from the five students who worked at Mining 3 in 2018 are available to the current students. This allows previous designs to be learned from and improved upon.
$10,000 budget	Mining 3 provided. $10,000 has been set aside for ordering any materials/components related to the autonomous hauler project.
Supervisors	I have two supervisors available to me (Erik Isokangas and Chandima Ekanayake) who are willing to answer any technical questions I may have related to my project.
Mining 3 Engineers	At Mining 3 there are numerous qualified engineers who are willing to answer questions and discuss ideas about the project.

Table 8: Necessary Resources for Project Completion

Appendix B.4: Project Opportunities

1. A possibility is that the proof of concept is successful and Mining 3 will continue to invest in the project. This could provide an opportunity to continue working on the autonomous hauler project at Mining 3 after the placement finishes in June 2019.

2. If the final output from this project is easy to up-scale, then the project will likely proceed to a larger prototype vehicle. A large scale working prototype will attract the attention of investors in the future.

3. Integrating autonomous vehicles into the mining industry will improve safety, since no personnel are being put at risk. This will serve as a strong selling point for the product.

Appendix C: Resonance Tuning Finite State Machine

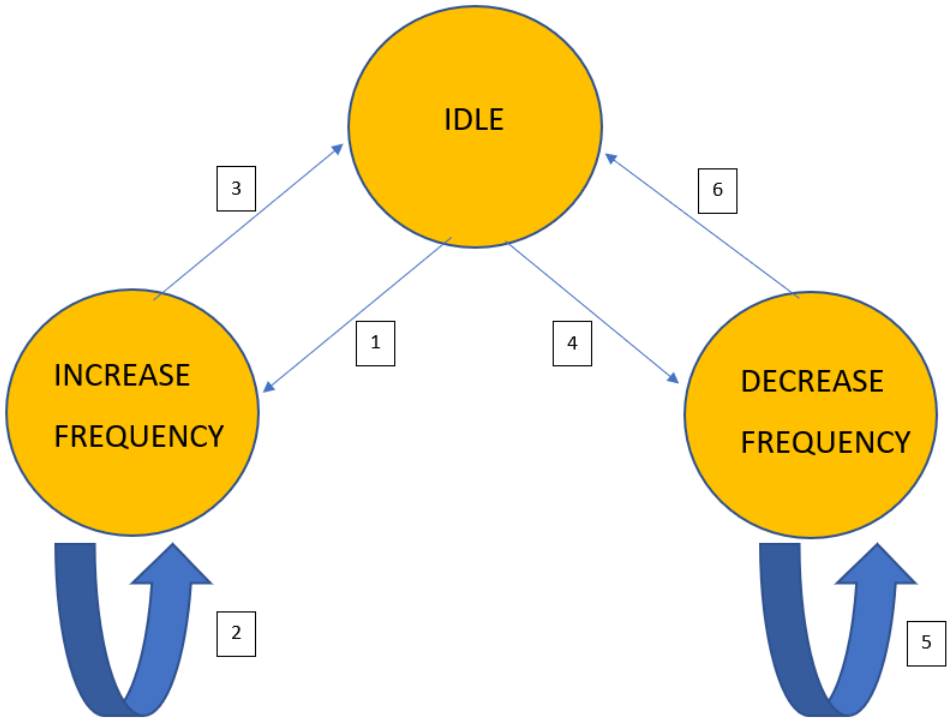

1. If the current state is IDLE, and the increase flag is TRUE, take path 1.

2. If the ADC voltage is larger than before after increasing the frequency, stay in the INCREASE FREQUENCY state by taking path 2.

3. If the ADC voltage is smaller than before or unchanged after increasing the frequency, return to IDLE state by taking path 3. Set increase flag to FALSE.

4. If the current state is IDLE, and the increase flag is FALSE, take path 4.

5. If the ADC voltage is larger than before after decreasing the frequency, stay in the DECREASE FREQUENCY state by taking path 5.

6. If the ADC voltage is smaller than before or unchanged after decreasing the frequency, return to IDLE state by taking path 6. Set increase flag to TRUE.

Appendix D: Finite State Machine TIVA Code

```
/*
 * Finite state machine to tune the frequency based on
 * the ADC readings.
 */
void run_ADC_fsm(struct ADC *adc) {

    // run current ADC fsm state
    switch(adc->state) {

        case IDLE:

            (adc->previous_adc_average) = (adc->current_adc_average);

            // get average adc value from 'n' samples (n determined by NUM_OF_ADC_SAMPLES)
            (adc->current_adc_average) = get_ADC_average();

            // If increase flag is true, switch state to INCREASE_FREQUENCY
            if (adc->increase) {
                (adc->state) = INCREASE_FREQUENCY;
            } else {
                (adc->state) = DECREASE_FREQUENCY;
            }
            break;

        case INCREASE_FREQUENCY:
            // If ADC voltage has increased, increase the frequency again
            if ((adc->current_adc_average) > ((adc->previous_adc_average) + ADC_SIGNIFICANT_CHANGE)) {
                change_frequency(adc);
            // If ADC voltage has not increased or has reduced, return to idle state and switch increase flag to FALSE
            } else {
                (adc->increase) = false;
                (adc->state) = IDLE;
            }
            break;

        case DECREASE_FREQUENCY:
            // If ADC voltage has increased, decrease the frequency again
            if ((adc->current_adc_average) > ((adc->previous_adc_average) + ADC_SIGNIFICANT_CHANGE)) {
                change_frequency(adc);
            // If ADC voltage has not increased or has reduced, return to idle state and switch increase flag to TRUE
            } else {
                (adc->increase) = true;
                (adc->state) = IDLE;
            }
            break;
    }
}
```